PHYSICAL REVIEW E **88**, 032918 (2013)

Analysis of a solvable model of a phase oscillator network on a circle with infinite-range Mexican-hat-type interaction

Tatsuya Uezu,[1,*] Tomoyuki Kimoto,[2] and Masato Okada[3]
[1]*Graduate School of Humanities and Sciences, Nara Women's University, Nara 630-8506, Japan*
[2]*Oita National College of Technology, Oita 870-0152, Japan*
[3]*Graduate School of Frontier Sciences, The University of Tokyo, Kashiwa, Chiba 277-8561, Japan*
(Received 15 October 2012; revised manuscript received 29 April 2013; published 27 September 2013)

We study a phase oscillator network on a circle with an infinite-range interaction. First, we treat the Mexican-hat interaction with the zeroth and first Fourier components. We give detailed derivations of the auxiliary equations for the phases and self-consistent equations for the amplitudes. We solve these equations and characterize the nontrivial solutions in terms of order parameters and the rotation number. Furthermore, we derive the boundaries of the bistable regions and study the bifurcation structures in detail. Expressions for location-dependent resultant frequencies and entrained phases are also derived. Secondly, we treat a different interaction that is composed of mth and nth Fourier components, where $m < n$, and we study its nontrivial solutions. In both cases, the results of numerical simulations agree quite well with the theoretical results.

DOI: 10.1103/PhysRevE.88.032918 PACS number(s): 05.45.Xt, 05.20.−y, 87.10.Rt

I. INTRODUCTION

Synchronization phenomena are ubiquitous in nature, and they are very important to living organisms. Typical examples include the simultaneous emission of light by fireflies, the rhythm of the heart composed of a population of cardiac muscle cells, and circadian rhythms [1,2].

Pioneering studies on such behavior were done by Winfree [3] and Kuramoto [4]. In particular, Kuramoto regarded synchronization as a phase transition and devised a model in which synchronization occurs as a phase transition in a nonequilibrium system. In general, when nonlinear dynamical systems with stable limit cycle oscillators are weakly coupled, the whole system can be described in terms of the phases of the oscillators, and the dynamical equation reduces to the evolution equation for phases [4]. Kuramoto proposed the so-called Kuramoto model, which is a coupled phase oscillator network. He found that the synchronization-desynchronization phase transition takes place when the system parameter reaches a certain value, and he derived an analytic expression for the critical point [5]. Since Kuramoto's analysis of globally coupled oscillators, oscillator networks with both short-range and intermediate-range interactions have been studied [6]. Oscillators with global and random interactions [7] and with sparse and random interactions [8] have also been studied. Moreover, a number of studies have analyzed the stability of the stationary states [9–11]. Many of these studies use the Fokker-Planck equation to derive a phase distribution density function with or without external noise. In particular, Otto and Antonsen derived evolution equations for the order parameters by assuming a special form for the Fourier components of the phase distribution density function [12]. Since this study, many studies have been published on the dynamical behavior of order parameters [13,14]. One of the interesting findings is the so-called Chimera state, in which some fraction of the oscillators are perfectly synchronized while the remainder are desynchronized [15–17]. Another topic on general coupled oscillator networks is noise-induced synchronization. It has been found that two identical nonlinear oscillators synchronize in the presence of common external Gaussian noise [18]. The findings of this study have been extended to include systems with common and oscillator-dependent noise [19,20], noise in the form of random impulses [21], and common noise consisting of only two values [22]. A review of the Kuramoto model and its extensions is available elsewhere [23]. There have also been extensive studies on the statistical and dynamical properties of the mean-field XY model (HMF XY model) of conservative dynamical systems that are related to oscillator network models of dissipative dynamical systems [24,25].

In our previous study [26], we investigated global coupled phase oscillators arranged on a circle. The interaction between two elements depended on their distance. In particular, we studied the Mexican-hat interaction, which is used in neuroscience studies to model feature extraction cells in the visual cortex and embodies the property that a firing cell excites nearby cells and inhibits distant cells [27]. The interaction is composed of the zeroth and first Fourier components. We proposed a method to derive auxiliary equations that enable us to determine the phases of three complex order parameters completely. By using these phases, we obtained expressions for the self-consistent equations (SCEs) of the amplitude of the order parameters and equations for the boundaries of the bistable regions. We performed numerical simulations and found that they agreed quite well with the theoretical results.

In this study, first we treat the interaction with the zeroth and first Fourier components. We call the Mexican-hat interaction model 1. This model was studied previously. In this paper, we give a derivation of the auxiliary equations for the phases and self-consistent equations for the amplitudes, solve these equations, and derive the boundaries of the bistable regions. We obtain three nontrivial solutions that are characterized by the order parameters and the rotation numbers of the synchronized oscillators. We draw the phase diagram by using formulas for the phase boundaries derived using the unstable pendulum (Pn) solution. We find that the disappearance of coexistent regions between the U and S solutions and between the

*uezu@ki-rin.phys.nara-wu.ac.jp

Pn and S solutions is due to the unstable solution and the stable solution annihilating each other. This type of transition does not exist in the Kuramoto model. We also analytically derive the location-dependent distribution of the resultant frequencies and entrained phases and validate the theoretical results by simulation, except for the chaotic behavior of the desynchronized oscillators. Secondly, we treat a different interaction with the mth and nth Fourier components, where $m < n$. We call this interaction model 2. We find the mth and nth spinning solutions, S_m and S_n, and a pendulum solution, Pn. We performed numerical simulations for the case of $m = 1$ and $n = 2$, and they confirmed the theoretical results.

The structure of this paper is as follows. From Secs. II–VI, we study model 1. In Sec. II, we formulate the problem and describe the SCEs and auxiliary equations. The solutions of the auxiliary equations are also given. In Sec. III, we characterize the nontrivial solutions by introducing the rotation number. In Sec. IV, we give the SCEs for the nontrivial solutions. The phase diagram and bifurcation structure are studied in Sec. V. In Sec. VI, we show the results of numerical simulations and compare them with the theoretical results. In Sec. VII, we study model 2 and show theoretical and numerical results for it. Section VIII contains a summary and discussion of the results. In Appendix A, we derive the auxiliary equations and SCEs for model 1 and solve the auxiliary equations. In Appendix B, we derive the SCEs and relevant quantities for each phase. In Appendix C, we derive the condition for the existence of the Pn solution. The expressions for the phase boundaries are derived in Appendix D. Appendix E derives the SCEs for the spinning and pendulum solutions for model 2.

II. FORMULATION

Let us consider N equally spaced phase oscillators lying on a circle. We introduce the coordinate θ on the circle, which takes values $0, \frac{2\pi}{N}, \frac{4\pi}{N}, \ldots, \frac{2(N-1)\pi}{N}$. Let ϕ_θ be the phase of the oscillator at the coordinate θ, and assume that it obeys the following differential equation:

$$\frac{d}{dt}\phi_\theta = \omega_\theta + \sum_{\theta'} J_{\theta,\theta'} \sin(\phi_{\theta'} - \phi_\theta). \quad (1)$$

Here, ω_θ is the natural frequency, and it is drawn from a probability density $g(\omega)$. $g(\omega)$ is assumed to be one-humped at $\omega = \omega_0$ and symmetric with respect to ω_0. The interaction $J_{\theta,\theta'}$ between oscillators at θ and θ' is assumed to be

$$J_{\theta,\theta'} = \frac{J_0}{N} + \frac{J_1}{N}\cos(\theta - \theta'). \quad (2)$$

This interaction has the properties of the Mexican-hat interaction described above. Now, let us introduce three complex order parameters,

$$W = Re^{i\Theta} = \frac{1}{N}\sum_\theta e^{i\phi_\theta}, \quad (3)$$

$$W_c = R_c e^{i\Theta_c} = \frac{1}{N}\sum_\theta \cos\theta\, e^{i\phi_\theta}, \quad (4)$$

$$W_s = R_s e^{i\Theta_s} = \frac{1}{N}\sum_\theta \sin\theta\, e^{i\phi_\theta}. \quad (5)$$

By using these quantities, the evolution equation (1) can be rewritten as

$$\frac{d}{dt}\phi_\theta = \omega_\theta + J_0 R\sin(\Theta - \phi_\theta) + J_1[R_c\cos\theta\sin(\Theta_c - \phi_\theta) + R_s\sin\theta\sin(\Theta_s - \phi_\theta)]. \quad (6)$$

Let us study the stationary states of this equation. Since oscillators with a natural frequency ω_0 are the most numerous, it is expected that the phases of the order parameters rotate with the frequency ω_0 in the stationary states. Thus, we will assume the following relations:

$$\Theta = \omega_0 t + \Theta', \quad \Theta_c = \omega_0 t + \Theta_c', \quad \Theta_s = \omega_0 t + \Theta_s'.$$

Since we are studying stationary states, we will assume that the amplitudes R, R_c, R_s and the phases $\Theta', \Theta_c', \Theta_s'$ tend to constant values as t goes to infinity. We could assume $\omega_0 = 0$ without loss of generality. However, we will retain the term ω_0 because the parameters at critical points explicitly contain ω_0.

Now, let us derive the SCEs following Kuramoto's argument. We rewrite the right-hand side of Eq. (6) as

$$\frac{d}{dt}\phi_\theta = \omega_\theta - A_\theta\sin(\phi_\theta - \omega_0 t - \alpha_\theta). \quad (7)$$

From Eqs. (6) and (7), the following relation is derived:

$$A_\theta e^{i\alpha_\theta} = J_0 R e^{i\Theta'} + J_1[R_c\cos\theta e^{i\Theta_c'} + R_s\sin\theta e^{i\Theta_s'}]. \quad (8)$$

For simplicity, we will omit primes from the phases except for the expressions of α_θ and ϕ_θ^*. A_θ is expressed as

$$\begin{aligned} A_\theta^2 = {} & (J_0R)^2 + J_1^2\{(R_c\cos\theta)^2 + (R_s\sin\theta)^2 \\ & + 2R_cR_s\cos(\Theta_c - \Theta_s)\sin\theta\cos\theta\} \\ & + 2J_0J_1R\{R_c\cos(\Theta_c - \Theta)\cos\theta \\ & + R_s\cos(\Theta_s - \Theta)\sin\theta\}. \end{aligned} \quad (9)$$

Since we assume that Θ's and R's do not depend on time, neither does α_θ. Thus, by defining $\psi_\theta \equiv \phi_\theta - \omega_0 t - \alpha_\theta$, the evolution equation becomes

$$\frac{d}{dt}\psi_\theta = \omega_\theta - \omega_0 - A_\theta\sin\psi_\theta. \quad (10)$$

A. Synchronized oscillators: $|\omega_\theta - \omega_0| \leqslant A_\theta$

The stable and unstable solutions are as follows:

$$\text{Stable solutions: } 0 < \psi_\theta < \frac{\pi}{2} \quad \text{for} \quad \omega_\theta - \omega_0 > 0$$
$$\text{and } -\frac{\pi}{2} < \psi_\theta < 0 \quad \text{for} \quad \omega_\theta - \omega_0 > 0,$$
$$\text{Unstable solutions: } \frac{\pi}{2} < \psi_\theta < \pi \quad \text{for} \quad \omega_\theta - \omega_0 > 0$$
$$\text{and } -\pi < \psi_\theta < -\frac{\pi}{2} \quad \text{for} \quad \omega_\theta - \omega_0 > 0.$$

The entrained phase ψ_θ^* and number density of the synchronized oscillators with phase ψ at the location θ, $n_s(\theta,\psi)$ are obtained as

$$\psi_\theta^* = \sin^{-1}\left(\frac{\omega_\theta - \omega_0}{A_\theta}\right), \quad (11)$$

$$n_s(\theta,\psi) = g(\omega_0 + A_\theta\sin\psi)A_\theta\cos\psi, \quad |\psi| \leqslant \frac{\pi}{2}, \quad (12)$$

where $\sin^{-1}(x)$ is assumed to be the principal value and its range is $[-\frac{\pi}{2},\frac{\pi}{2}]$.

B. Desynchronized oscillators: $|\omega_\theta - \omega_0| > A_\theta$

The solution of Eq. (10) is

$$\psi_\theta(t) = \tilde{\omega}'_\theta t + h(\tilde{\omega}'_\theta t),$$

where $h(t)$ is a periodic function of t with period 2π. $\tilde{\omega}'_\theta$ is the resultant frequency given by

$$\tilde{\omega}'_\theta = (\omega_\theta - \omega_0)\sqrt{1-\left(\frac{A_\theta}{\omega_\theta-\omega_0}\right)^2}.$$

The solution of Eq. (7) is

$$\phi_\theta(t) = \omega_0 t + \psi_\theta(t) + \alpha_\theta.$$

Therefore, the resultant frequency $\tilde{\omega}_\theta$ for $\phi_\theta(t)$ is

$$\tilde{\omega}_\theta = \omega_0 + \tilde{\omega}'_\theta = \omega_0 + (\omega_\theta - \omega_0)\sqrt{1-\left(\frac{A_\theta}{\omega_\theta-\omega_0}\right)^2}. \quad (13)$$

The probability density function of the phase of desynchronized oscillators at location θ, $p_{\rm ds}(\theta,\psi)$, obeys the following equation:

$$\frac{\partial}{\partial\psi}((\omega_\theta - \omega_0 - A_\theta\sin\psi)p_{\rm ds}(\theta,\psi)) = 0.$$

Solving it yields

$$p_{\rm ds}(\theta,\psi) = \frac{|\omega_\theta-\omega_0|}{2\pi}\frac{1}{|\omega_\theta-\omega_0-A_\theta\sin(\psi)|}\times\sqrt{1-\left(\frac{A_\theta}{\omega_\theta-\omega_0}\right)^2}. \quad (14)$$

From this, the number density of desynchronized oscillators with phase ψ at θ, $n_{\rm ds}(\theta,\psi)$, can be written as

$$n_{\rm ds}(\theta,\psi) = \int_{|\frac{A_\theta}{\omega-\omega_0}|<1} g(\omega)p_{\rm ds}(\theta,\psi)d\omega = \frac{1}{\pi}\int_{A_\theta}^{\infty} dx\, x g(\omega_0+x)\frac{\sqrt{x^2-A_\theta^2}}{x^2-A_\theta^2\sin^2\psi}. \quad (15)$$

C. Resultant frequency distribution

We study the resultant frequency distribution for the synchronized and desynchronized oscillators at θ, $G_s(\tilde{\omega},\theta)$ and $G_{\rm ds}(\tilde{\omega},\theta)$. $G_s(\tilde{\omega},\theta)$ is

$$G_s(\tilde{\omega},\theta) = \frac{N_{\theta,s}}{N}\delta(\tilde{\omega}-\omega_0), \quad (16)$$

where $N_{\theta,s}d\theta$ is the number of synchronized oscillators located in $(\theta,\theta+d\theta)$, and $\delta(x)$ is the Dirac delta. $G_{\rm ds}(\tilde{\omega},\theta)$ is expressed as

$$G_{\rm ds}(\tilde{\omega},\theta) = \frac{|\tilde{\omega}-\omega_0|}{\sqrt{(\tilde{\omega}-\omega_0)^2+A_\theta^2}}g\left[\omega_0+\sqrt{(\tilde{\omega}-\omega_0)^2+A_\theta^2}\right]. \quad (17)$$

The following relation is used in the derivation:

$$\omega_\theta = \omega_0 + (\tilde{\omega}_\theta - \omega_0)\sqrt{1+\left(\frac{A_\theta}{\tilde{\omega}_\theta-\omega_0}\right)^2}. \quad (18)$$

D. SCEs, auxiliary equations, and solutions of auxiliary equations

In this subsection, we state the SCEs, the auxiliary equations, and the solutions of the auxiliary equations. Their derivations are in Appendix A.

Here, we will introduce the following notation:

$$\langle B\rangle \equiv \frac{1}{Z}\frac{1}{\pi}\int_0^{\pi/2}d\psi\int_0^{2\pi}d\theta\, g(\omega_0+A_\theta\sin\psi)\cos^2\psi\; B, \quad (19)$$

$$Z \equiv \frac{1}{\pi}\int_0^{\pi/2}d\psi\int_0^{2\pi}d\theta\, g(\omega_0+A_\theta\sin\psi)\cos^2\psi. \quad (20)$$

The SCEs are

$$R = (J_0R + J_1\{R_c\langle\cos\theta\rangle\cos(\Theta_c-\Theta) + R_s\langle\sin\theta\rangle\cos(\Theta_s-\Theta)\})Z, \quad (21)$$

$$R_c = (J_0R\langle\cos\theta\rangle\cos(\Theta_c-\Theta) + J_1\{R_c\langle\cos^2\theta\rangle + R_s\langle\sin\theta\cos\theta\rangle\cos(\Theta_c-\Theta_s)\})Z, \quad (22)$$

$$R_s = (J_0R\langle\sin\theta\rangle\cos(\Theta_s-\Theta) + J_1\{R_c\langle\sin\theta\cos\theta\rangle \times\cos(\Theta_c-\Theta_s) + R_s\langle\sin^2\theta\rangle\})Z. \quad (23)$$

The auxiliary equations are

$$R_c\langle\cos\theta\rangle\sin(\Theta_c-\Theta) + R_s\langle\sin\theta\rangle\sin(\Theta_s-\Theta) = 0, \quad (24)$$

$$J_0R\langle\cos\theta\rangle\sin(\Theta_c-\Theta) + J_1R_s\langle\sin\theta\cos\theta\rangle\sin(\Theta_c-\Theta_s) = 0, \quad (25)$$

$$J_0R\langle\sin\theta\rangle\sin(\Theta_s-\Theta) - J_1R_c\langle\sin\theta\cos\theta\rangle\sin(\Theta_c-\Theta_s) = 0. \quad (26)$$

Two of the auxiliary equations are independent. Thus, the phases of the complex order parameters are completely determined from the auxiliary equations. We list their solutions below.

(i) $R=0, R_1\equiv\sqrt{R_c^2+R_s^2}\neq 0$. $\cos(\Theta_c-\Theta_s)=0$, that is, $\Theta_c-\Theta_s=\pm\frac{\pi}{2}$ (mod 2π). This corresponds to the stable spinning (S) solution.

(ii) $R\neq 0, R_1\neq 0$.

A $\sin(\Theta_c-\Theta_s)=0$ and $\cos(\Theta_c-\Theta)=0$, that is, $\{\Theta_c-\Theta,\Theta_s-\Theta\} = \{\pm\frac{\pi}{2}$ (mod 2π), $\pm\frac{\pi}{2}$ (mod 2π)$\}$. This corresponds to the stable pendulum (Pn) solution.

B $\sin(\Theta_c-\Theta)=0$ and $\cos(\Theta_s-\Theta)=0$, that is, $\{\Theta_c-\Theta,\Theta_s-\Theta\} = \{0$ or π (mod 2π), $\pm\frac{\pi}{2}$ (mod 2π)$\}$. This corresponds to the unstable Pn solution.

Hereafter, we omit "(mod 2π)" for simplicity.

III. CHARACTERIZATION OF THE SOLUTIONS

The preceding section determined the phases of the order parameters from the auxiliary equations. Furthermore,

Appendix B derives four solutions of the SCEs. These solutions are classified on the basis of the values of R and R_1:

P: paramagnetic solution, $(R,R_1) = (0,0)$,

U: uniform solution, $(R,R_1) = (+,0)$,

S: spinning solution, $(R,R_1) = (0,+)$, $\quad (\Theta_c - \Theta_s) = \pm\frac{\pi}{2}$,

Pn: pendulum solution, $(R,R_1) = (+,+)$,

$$\{\Theta_c - \Theta, \Theta_s - \Theta\} = \left\{\pm\frac{\pi}{2}, \pm\frac{\pi}{2}\right\}. : \text{ stable},$$

$$\{\Theta_c - \Theta, \Theta_s - \Theta\} = \left\{0 \text{ or } \pi, \pm\frac{\pi}{2}\right\}. : \text{ unstable}.$$

Let us study the physical meanings of these solutions. To characterize them, we will define the rotation number of a solution. Let us denote an oscillator at θ as XY spin $\boldsymbol{X}_\theta = (\cos\phi_\theta, \sin\phi_\theta)$ in the two-dimensional space. We focus on the behavior of synchronized oscillators with entrained phases $\phi^*_\theta = \omega t + \psi^*_\theta + \alpha_\theta$. The rotation number is the number of rotations of a synchronized oscillator $\boldsymbol{X}^*_\theta = (\cos\phi^*_\theta, \sin\phi^*_\theta)$ around the origin in the space $\boldsymbol{X}$ when the location θ changes by 2π. We define the rotation as being positive (negative) when the rotation is anticlockwise (clockwise). In the P solution, all oscillators desynchronize, whereas in the other three solutions, an extensive number of oscillators synchronize and their directions become locked. We depict θ dependencies of the entrained phase ϕ^*_θ for each solution in Figs. 1(a)–1(c). Although ϕ^*_θ fluctuates in all solutions, the behavior of ϕ^*_θ together with the rotation number characterize each solution. In the U solution, ϕ^*_θ randomly takes on a value in the interval $[-\frac{\pi}{2} + \Theta, \frac{\pi}{2} + \Theta]$ irrespective of the location of oscillators; hence, the rotation number is 0. In the S solution, ϕ^*_θ linearly depends on θ, and the rotation number is ± 1. See Appendix B for the derivations of these solutions. In the Pn solution, ϕ^*_θ has an oscillatory behavior and the rotation number is 0, but the directions of neighboring synchronized oscillators are weakly correlated.

IV. SELF-CONSISTENT EQUATIONS FOR ORDERED SOLUTIONS

This section uses the same notation as in Sec. II; that is, Θ's denote Θ''s. We give the SCEs and relevant quantities of various solutions of the SCEs. The derivations are given in Appendix B.

A. Stable U solution

In the U solution, $R_1 = 0$. This is merely the solution of the Kuramoto model,

$$\begin{aligned} R &= 2J_0 R \int_0^{\pi/2} d\psi\, g(\omega_0 + J_0 R \sin\psi)\cos^2\psi, \\ A_\theta &= J_0 R, \quad \alpha_\theta = \Theta' = \text{const}, \\ \phi^*_\theta &= \omega_0 t + \Theta' + \sin^{-1}\left(\frac{\omega_\theta - \omega_0}{J_0 R}\right). \end{aligned} \tag{27}$$

The phase transition point from the P phase to the U phase is

$$J_{0,c} = \frac{2}{\pi g(\omega_0)}. \tag{28}$$

B. Stable S solution

For the stable S solution, $R = 0$, $\langle\cos\theta\rangle = \langle\sin\theta\rangle = 0$, and $\Theta_c - \Theta_s = \pm\frac{\pi}{2}$,

$$\begin{aligned} R_c &= J_1 R_c \int_0^{\pi/2} d\psi\, g(\omega_0 + J_1 R_c \sin\psi)\cos^2\psi, \\ R_c &= R_s = \frac{R_1}{\sqrt{2}}, \quad A_\theta = J_1 R_c, \alpha_\theta = \Theta'_c \mp \theta, \\ \phi^*_\theta &= \omega_0 t + \sin^{-1}\left(\frac{\omega_\theta - \omega_0}{J_1 R_c}\right) + \Theta'_c \mp \theta. \end{aligned} \tag{29}$$

The phase transition point from the P phase to the S phase and the order parameter R_1 near the transition point are

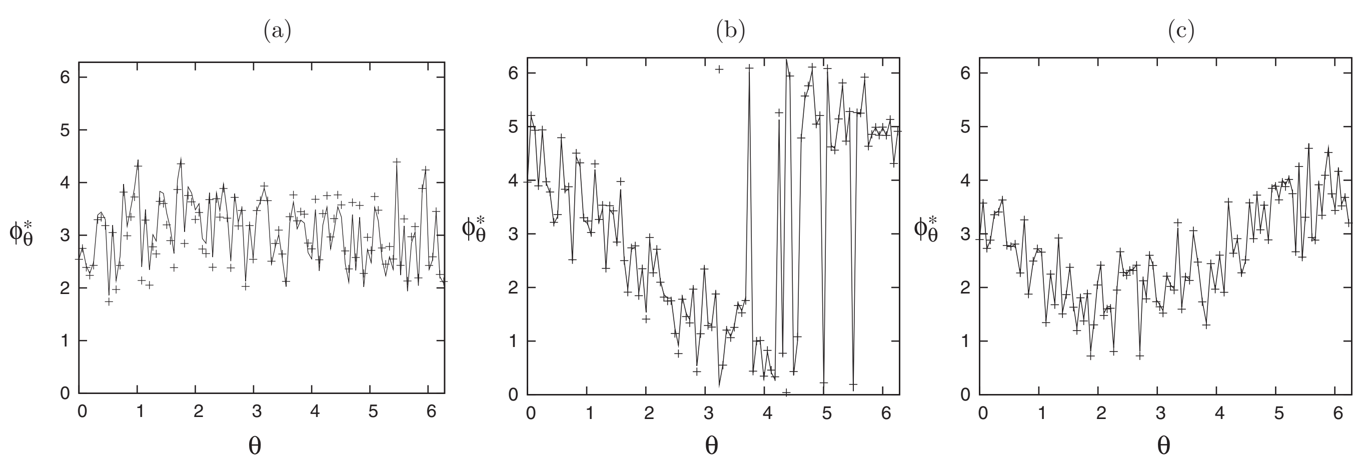

FIG. 1. θ dependencies of entrained phase ϕ^*_θ. Line plots: theory; +: simulation ($N = 10\,000$, $\sigma = 0.2$, $J_0 = 1.2 J_{0,c}$, $\omega_0 = 0$). Since ω_0 is 0, the theoretical values are calculated by using Eq. (11). These values are connected by straight lines so that it is easier to compare them with the numerical results. Only 1% of the entrained phases are depicted. (a) U solution, $J_1/J_0 = 1.9$; (b) S solution, $J_1/J_0 = 2.1$; (c) Pn solution, $J_1/J_0 = 2.1$.

given by

$$J_{1,c} = \frac{4}{g(\omega_0)\pi} = 2J_{0,c},$$
$$R_1 \simeq \frac{4}{J_{1,c}^2}\sqrt{\frac{2(J_1 - J_{1,c})}{\pi|g''(\omega_0)|}} \propto \sqrt{J_1 - J_{1,c}}. \quad (30)$$

When $g(\omega)$ is a Gaussian distribution with mean ω_0 and standard deviation σ, $J_{0,c}$ and $J_{1,c}$ become

$$J_{0,c} = 2\sqrt{\frac{2}{\pi}}\sigma, \quad J_{1,c} = 4\sqrt{\frac{2}{\pi}}\sigma = 2J_{0,c}.$$

The entrained phase ϕ_θ^* linearly depends on θ. Since the resultant frequency distributions for the synchronized and desynchronized oscillators do not depend on θ, we denote them by $G_s(\tilde{\omega})$ and $G_{ds}(\tilde{\omega})$, respectively,

$$G_s(\tilde{\omega}) = \frac{N_s}{N}\delta(\tilde{\omega} - \omega_0), \quad (31)$$

$$G_{ds}(\tilde{\omega}) = \frac{|\tilde{\omega} - \omega_0|}{\sqrt{(\tilde{\omega} - \omega_0)^2 + (J_1 R_c)^2}} \times g[\omega_0 + \sqrt{(\tilde{\omega} - \omega_0)^2 + (J_1 R_c)^2}], \quad (32)$$

where N_s is the number of synchronized oscillators.

C. Stable Pn solution

We define the phase φ of (R_c, R_s) as

$$R_c = R_1 \cos\varphi, \quad R_s = R_1 \sin\varphi.$$

Furthermore, defining $\bar{\alpha}_\theta = \alpha_\theta - \Theta_c$, we have

$$A_\theta \cos\bar{\alpha}_\theta = J_1 R_1 \cos[\theta - \varphi\cos(\Theta_c - \Theta_s)],$$
$$A_\theta \sin\bar{\alpha}_\theta = -J_0 R \sin(\Theta_c - \Theta), \quad (33)$$
$$A_\theta = \sqrt{(J_0 R)^2 + (J_1 R_1)^2 \cos^2[\theta - \varphi\cos(\Theta_c - \Theta_s)]},$$

where $\sin(\Theta_c - \Theta) = \pm 1$ and $\cos(\Theta_c - \Theta_s) = \pm 1$. By transforming θ into $\theta' = \theta - \varphi\cos(\Theta_c - \Theta_s)$, the SCEs become

$$R = \frac{4J_0 R}{\pi}\int_0^{\pi/2} d\psi \int_0^{\pi/2} d\theta' \, g(\omega_0 + A_{\theta'+\varphi\cos(\Theta_c - \Theta_s)}\sin\psi) \times \cos^2\psi, \quad (34)$$

$$R_1 = \frac{4J_1 R_1}{\pi}\int_0^{\pi/2} d\psi \int_0^{\pi/2} d\theta' \, g(\omega_0 + A_{\theta'+\varphi\cos(\Theta_c - \Theta_s)}\sin\psi) \times \cos^2\psi\cos^2\theta', \quad (35)$$

$$A_{\theta'+\varphi\cos(\Theta_c - \Theta_s)} = \sqrt{(J_0 R)^2 + (J_1 R_1)^2\cos^2\theta'}, \quad (36)$$

$$\phi_\theta^* = \omega_0 t + \alpha_\theta + \sin^{-1}\left(\frac{\omega_\theta - \omega_0}{A_\theta}\right) = \omega_0 t + \bar{\alpha}_\theta + \Theta_c' + \sin^{-1}\left(\frac{\omega_\theta - \omega_0}{A_\theta}\right). \quad (37)$$

In the preceding equation, θ is the original coordinate and A_θ is given by Eq. (33). From (37), the rotation number is 0. Using this A_θ, the resultant frequency distributions $G_s(\tilde{\omega},\theta)$ and $G_{ds}(\tilde{\omega},\theta)$ are given by Eqs. (16) and (17).

D. Unstable Pn solution

Setting $\bar{\alpha}_\theta = \alpha_\theta - \Theta_c$, we have

$$A_\theta \sin\bar{\alpha}_\theta = -J_1 R_s \sin\theta\sin(\Theta_c - \Theta_s),$$
$$A_\theta \cos\bar{\alpha}_\theta = J_0 R\cos(\Theta_c - \Theta) + J_1 R_c\cos\theta,$$
$$A_\theta = \sqrt{[J_0 R\cos(\Theta_c - \Theta) + J_1 R_c\cos\theta]^2 + (J_1 R_s\sin\theta)^2}.$$

By transforming θ into $\theta' = \theta - (\Theta_c - \Theta)$, Eqs. (21), (22), and (23) become

$$R = \frac{2}{\pi}\int_0^{\pi/2} d\psi \int_0^{\pi} d\theta' g(\omega_0 + A_{\theta'+\Theta_c-\Theta}\sin\psi)\cos^2\psi \times (J_0 R + J_1 R_c\cos\theta'), \quad (38)$$

$$R_c = \frac{2}{\pi}\int_0^{\pi/2} d\psi \int_0^{\pi} d\theta' g(\omega_0 + A_{\theta'+\Theta_c-\Theta}\sin\psi)\cos^2\psi \times (J_0 R + J_1 R_c\cos\theta')\cos\theta', \quad (39)$$

$$R_s = J_1 R_c \frac{2}{\pi}\int_0^{\pi/2} d\psi \int_0^{\pi} d\theta' g(\omega_0 + A_{\theta'+\Theta_c-\Theta}\sin\psi) \times \cos^2\psi \, \sin^2\theta', \quad (40)$$

where $A_{\theta'+\Theta_c-\Theta} = \sqrt{(J_0 R + J_1 R_c\cos\theta')^2 + (J_1 R_s\sin\theta')^2}$.

By numerically solving Eqs. (34) and (35) for the stable Pn solution, we obtain the U solution by setting $R_1 = 0$ and the stable Pn solution by setting $R_1 \neq 0$. This is because Eq. (34) with $R_1 = 0$ reduces to the SCE (27) for the U solution. A necessary condition to obtain a stable Pn solution is $J_1 > 2J_0$. We prove this in Appendix C.

V. PHASE DIAGRAM AND BIFURCATION STRUCTURE

Figure 2(a) is the phase diagram in scaled parameter space $(J_0/\sigma, J_1/\sigma)$. Here, σ is the standard deviation of the Gaussian distribution $g(\omega)$ that was used in the simulations. The diagram shows that the S and U solutions can coexist and the S and Pn solutions can coexist. Figure 2(b) shows the J_1/σ dependencies of the order parameters R and R_1 with J_0/σ fixed to 4. From this figure, we can see that the Pn solution bifurcates from the U solution continuously, as is proved in Appendix C. On the other hand, the S solution bifurcates from the P solution at the critical value of J_1/σ. Furthermore, the unstable Pn solution and stable S solution merge and the stable S solution becomes unstable as J_1/σ decreases, and the unstable and stable Pn solutions merge and the stable Pn solution becomes unstable as J_1/σ increases. Therefore, the unstable Pn solution determines the boundary of the coexistent regions of the S and U solutions and of the S and Pn solutions. Taking into account these observations, we can derive the boundaries of the coexisting solutions by using the unstable Pn solution and relevant stable solutions. The equations for the boundaries are derived in Appendix D.

VI. NUMERICAL RESULTS

We performed numerical simulations using a Gaussian distribution with mean 0 and standard deviation σ as $g(\omega)$. That is, $\omega_0 = 0$. If J_0 or J_1 is large in the calculation, the discretization of $\frac{d\phi_i}{dt}$ by the Euler method, $\frac{\phi_i(t+h)-\phi_i(t)}{h}$, becomes worse [6]. Since the evolution equations with the same values

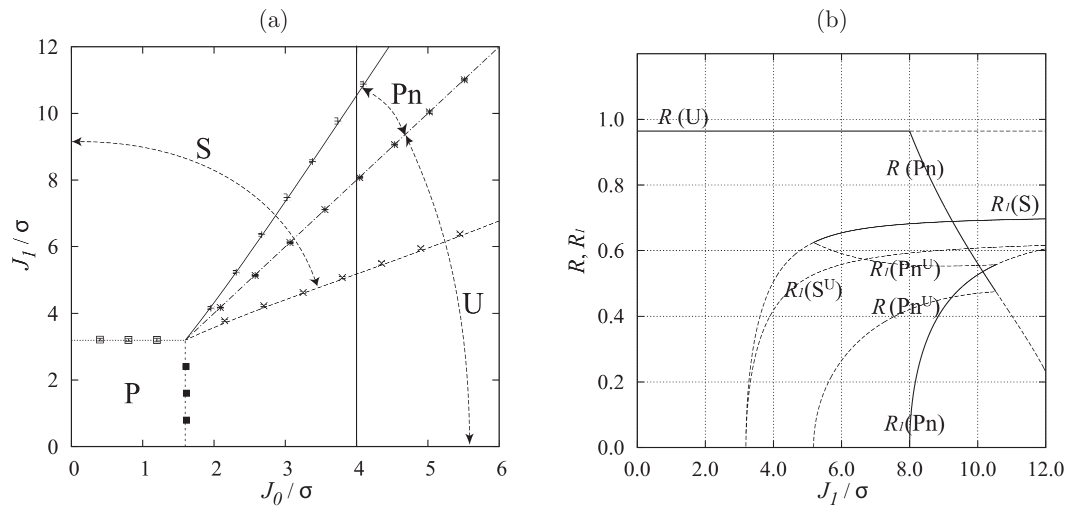

FIG. 2. (a) Phase diagram in scaled parameter space. Plotted points represent simulation results and curves represent theoretical results. The solid vertical line represents the parameters used to depict Fig. 2(b). (b) Bifurcation diagram, J_1/σ dependencies of the order parameters. $J_0/\sigma = 4$. Solid curves: stable solutions, dashed curves: unstable solutions, which have superscripts U, e.g., S^U.

of ω_0/σ, J_0/σ, and J_1/σ become identical by changing the time scale from t to σt, we fix J_0 or J_1 and change σ when J_0 or J_1 is large. The Euler method had a time increment $h = 0.1$.

A. Phase diagram

Figure 2(a) depicts the theoretically and numerically obtained boundaries. The theoretical results (the solid curves) are in good agreement with the simulation results (symbols). Now, let us examine the physical meanings of the phase transitions by using the rotation numbers of the solutions. There are five boundaries in the phase diagram shown in Fig. 2(a). The transition from the P to U phase takes place continuously at $J_0/\sigma = (J_0/\sigma)_c$ for $0 \leqslant J_1/\sigma \leqslant (J_1/\sigma)_c$, and this is the same transition as in the Kuramoto model. The transition from the P to S phase takes place continuously at $J_1/\sigma = (J_1/\sigma)_c \equiv 2(J_0/\sigma)_c$ for $0 \leqslant J_0/\sigma \leqslant (J_0/\sigma)_c$. In the P phase, there are no synchronized oscillators and the rotation number is not defined. In the S phase, the rotation number is 1. The above illustrates that a solution with a nonzero rotation number can appear from a solution in which the rotation number is not defined. Another example of this occurs in model 2 (see Sec. VIII). That is, the S_m solution with the rotation number $\pm m$ appears from the P solution when the mth Fourier component exists in the interaction. The transition from the U to Pn phase takes place continuously at $J_1/\sigma = 2J_0/\sigma$ for $J_0/\sigma \geqslant (J_0/\sigma)_c$ and $J_1/\sigma \geqslant (J_1/\sigma)_c$. In this case, the rotation number of the U and Pn phases is 0. This is reasonable because the transition is continuous and synchronized oscillators exist in both phases. Although both solutions have the same rotation number, 0, they are different. That is, as is shown in Figs. 1(a) and 1(c), the directions of the two synchronized oscillators do not correlate in the U phase, but they correlate weakly in the Pn phase. Now, let us investigate the transitions at the bistable region boundaries. As mentioned in the previous section, the stable S and unstable Pn solutions merge and the stable S solution disappears at the boundary between the S and U solutions, and the stable Pn and unstable Pn solutions merge and the stable Pn solution disappears at the boundary between the S and Pn solutions. This type of transition does not exist in the Kuramoto model. When the stable S solution with rotation number ± 1 and the unstable Pn solution merge, these two solutions should have the same rotation number, ± 1. Likewise, when the stable Pn solution with rotation number 0 and the unstable Pn solution merge, their rotation numbers should be 0. Thus, the rotation number of the unstable Pn solution changes from ± 1 to 0 as J_1/σ increases. This is really the case, as evidenced by Fig. 3. When we calculated ϕ_θ^* for the unstable solution, we assumed $\Theta_c = 0$, $\Theta_c - \Theta = 0$, and $\Theta_s - \Theta = \pi/2$, and we fixed these values when values of J_1/σ change, because these phases take on discrete values and are considered to be continuous with respect to the system parameters. The reason why the rotation number can change as a system parameter changes is as follows. Oscillators are discretely spread out on a circle and the difference between the phases of the neighboring synchronized oscillators can become π. Since the phase difference is defined in mod 2π, if it changes and takes on the value π, the rotation number will change by ± 1. The rotation number is not defined if there are neighboring synchronized oscillators whose phases differ by π. However, this situation is very special. In most cases, it is defined and can be used to classify solutions and get physical information on them.

B. Spinning solution

Figures 4(a) and 4(b) plot the dependence of R_1 and the distribution of the resultant frequencies $G(\tilde{\omega})$ on $\frac{\sigma}{J_1}$. The location-dependent entrained phase ϕ_θ^* is in Fig. 1(b). It turns out that the entrained phase depends linearly on θ in the S solution but takes on random values for the U solution [see Fig. 1(b)], as theoretically expected. All of the numerical results agree quite well with the theoretical results.

C. Pendulum solution

Figure 5 displays the theoretical and simulated results of the J_0 dependence of the order parameters for $J_1 = 2.1J_0$. The

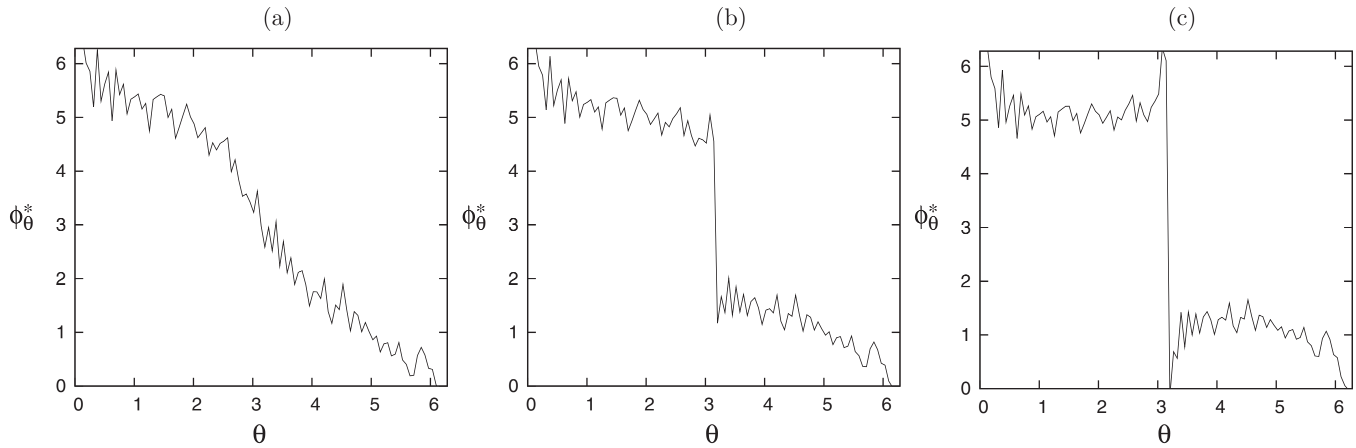

FIG. 3. Theoretical estimation of θ dependencies of phases ϕ^*_θ for unstable Pn solution. $\sigma = 0.2$, $J_0/\sigma = 4$. The theoretical values are calculated using a similar equation to Eq. (11) for the unstable Pn solution, and these values are connected by straight lines. Only 1% of the phases are depicted. (a) $J_1/\sigma = 6$, near the boundary of the region in which the S and U phases coexist; (b) $J_1/\sigma = 8$, at the boundary of the region in which the S and U phases coexist; (c) $J_1/\sigma = 10$, near the boundary of the region in which the S and Pn phases coexist.

theoretical and simulation results of the location-dependent resultant frequency distribution $G(\tilde{\omega},\theta)$ for different θ are in Fig. 6, and those of the θ dependencies of the entrained phases ϕ^*_θ are in Fig. 1(c). The agreement between the theoretical and numerical results is excellent. To investigate the desynchronized oscillators, we constructed a Lorenz plot of the time series $\sin[\phi_i(t)]$ for the Pn solution (Fig. 7).

The Lorenz plot is a mapping from the difference $\Delta t_l = t_{l+1} - t_l$ to Δt_{l+1}, where t_l and t_{l+1} are successive times that satisfy $\cos[\phi_i(t_l)] = 1$ and $\cos[\phi_i(t_{l+1})] = 1$, respectively. As shown in Fig. 7, the simulation results are scattered in the Lorenz plot. This indicates that the trajectory of a desynchronized oscillator behaves chaotically even though theoretically it is quasiperiodic. However, this is reasonable because synchronized and desynchronized oscillators interact with other oscillators, and desynchronized oscillators are easily influenced by perturbations, whereas entrained oscillators are forced to lock to the fixed phases. As is well known, quasiperiodic motion with more than two dimensions generically becomes chaotic through perturbation [28]. In most of our numerical results, e.g., those for the resultant frequency distribution, the larger N is, the better the agreement between the theoretical and numerical results becomes. These results suggest that the system behaves quasiperiodically as N goes to infinity.

VII. SYSTEM WITH INTERACTION COMPOSED OF FIRST AND SECOND FOURIER COMPONENTS

In this section, we study model 2, in which the interaction is given by

$$J_{\theta,\theta'} = \frac{1}{N}[J_m \cos\{m(\theta - \theta')\} + J_n \cos\{n(\theta - \theta')\}], \quad (41)$$

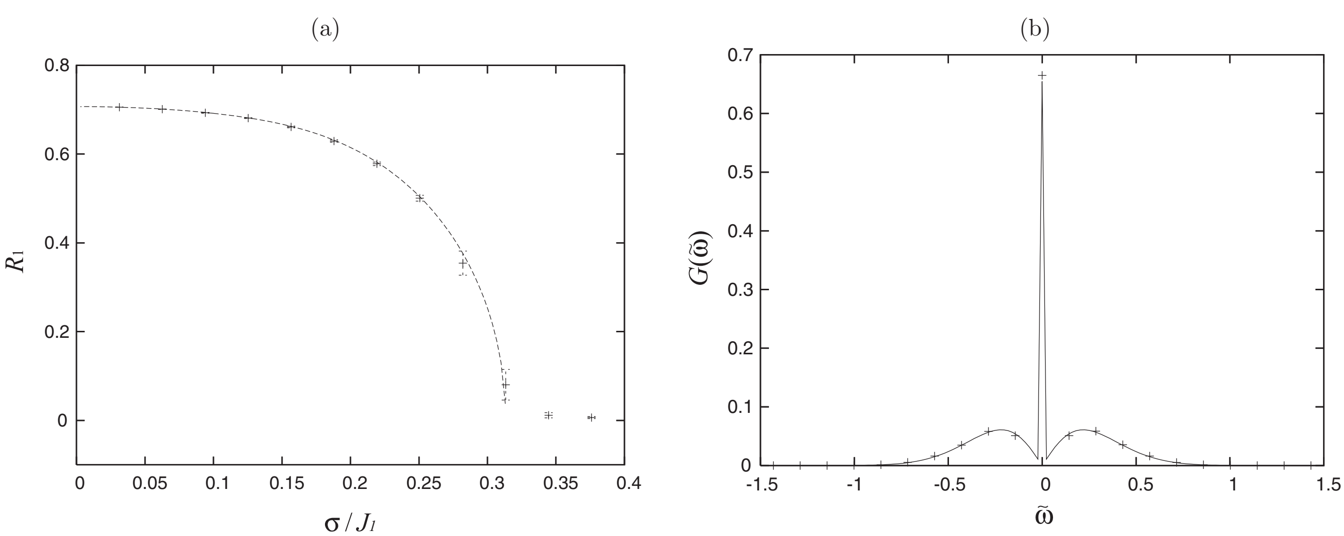

FIG. 4. (a) σ/J_1 dependence of R_1. $\sigma/J_1 = (\sigma/J_1)_c i$, $i = 0.1, 0.2, \ldots, 1.2$. We set $J_0 = 0$ and $J_1 = 1$ and change σ. We set $\omega_0 = 0$. Dashed curve: theory. Symbols: simulation. $N = 20\,000$. The sample average was taken over 20 initial configurations. Vertical lines are error bars. (b) The distribution of the resultant frequencies $G(\tilde{\omega})$ in the ordered phase calculated for a sample. $N = 100\,000$. Solid curve: theory. Symbols: simulation. $J_0 = 0, J_1 = 1$. $\sigma/J_1 = (\sigma/J_1)_c 0.9$.

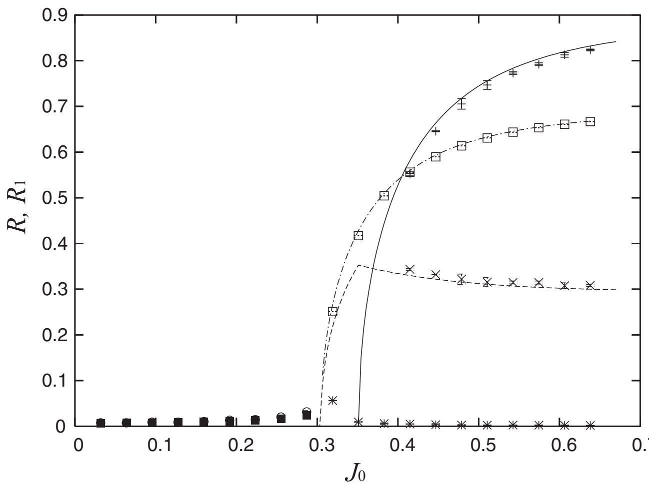

FIG. 5. J_0 dependencies of order parameters. $J_1 = 2.1J_0$. Curves: theory, symbols: simulation. $N = 20\,000$, $\sigma = 0.2$. Averages are taken from 20 samples. Solid curve and $+$: R of Pn solution, dashed curve and $\times$: R_1 of Pn solution, dashed-dotted curve and square: R_1 of S solution. Vertical lines are error bars. The error bars of almost all of the data are too small to see.

where m and n are positive integers, and we assume that $m < n$. The order parameters are defined as

$$R_{kc}e^{i\Theta_{kc}} = \frac{1}{N}\sum_{\theta}\cos(k\theta)e^{i\phi_\theta}, \tag{42}$$

$$R_{ks}e^{i\Theta_{ks}} = \frac{1}{N}\sum_{\theta}\sin(k\theta)e^{i\phi_\theta}. \tag{43}$$

k is m or n. As usual, we assume that R_{kc} and R_{ks} tend to be constant and $\Theta_{kc} \to \omega_0 t + \Theta'_{kc}, \Theta_{ks} \to \omega_0 t + \Theta'_{ks}$ as t tends to ∞, and Θ'_{kc} and Θ'_{kc} are constant. The evolution equation is given by

$$\begin{aligned}\frac{d}{dt}\phi_\theta &= \omega_\theta - A_\theta \sin(\phi_\theta - \omega_0 t - \alpha_\theta),\\ A_\theta e^{i\alpha_\theta} &= \sum_{k=m,n} J_k[R_{kc}\cos(k\theta)e^{i\Theta'_{kc}} + R_{ks}\sin(k\theta)e^{i\Theta'_{ks}}].\end{aligned} \tag{44}$$

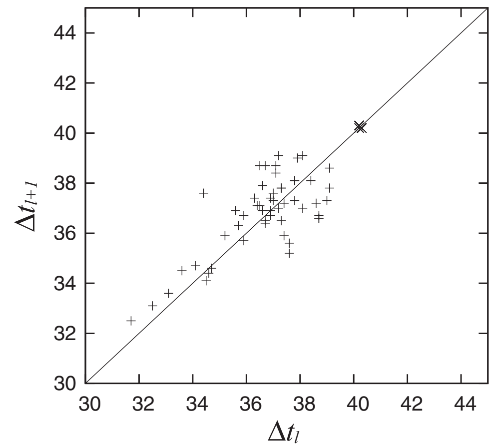

FIG. 7. Lorenz plot of desynchronized oscillator in Pn solution. $\times$: theory; $+$: simulation ($N = 10\,000$, $\sigma = 0.2$, $J_1/J_0 = 2.1$, $J_0 = 1.2J_{0,c}$).

Defining $\psi_\theta = \phi_\theta - \omega_0 t - \alpha_\theta$, the evolution equation becomes

$$\frac{d}{dt}\psi_\theta = \omega_\theta - \omega_0 - A_\theta \sin\psi_\theta. \tag{45}$$

For later use, we define R_k and φ_k by $R_{kc} + iR_{ks} = R_k e^{ik\varphi_k}$. In the next subsections, we give the SCE for the stable spinning and pendulum solutions. The derivations are in Appendix E. Below, for simplicity, we will omit primes from the phases except for the expressions of α_θ and ϕ^*_θ.

A. Spinning solution

We give the conditions and SCEs for the stable spinning solution with $R_m > 0$ and $R_n = 0$. We denote the solution by S_m. The conditions on this solution are $\cos(\Theta_{mc} - \Theta_{ms}) = 0$ and $\cos(2m\varphi_m) = 0$. From this, $R_{mc} = R_{ms} = \frac{1}{\sqrt{2}}R_1$ and $A_\theta = J_m R_{mc}$ follow. The SCE is

$$1 = J_m \int_0^{\pi/2} d\psi\, g(\omega_0 + J_m R_{mc}\sin\psi)\cos^2\psi. \tag{46}$$

(a) (b)

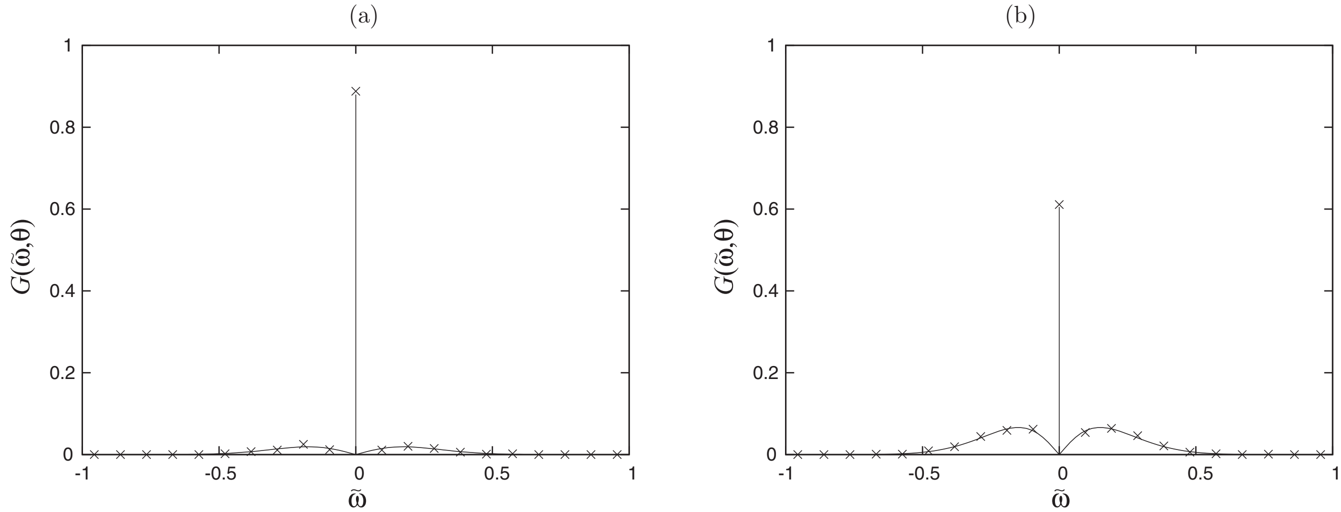

FIG. 6. Theoretical and simulated results for the distribution $G(\tilde{\omega},\theta)$ of the resultant frequencies for the Pn solution. Curve: theory, $+$: simulation ($N = 100\,000$, $\sigma = 0.2$, $J_1/J_0 = 2.1$, $J_0 = 1.2J_{0,c}$). (a) $\theta = 0.05 \times 2\pi$, (b) $\theta = 0.25 \times 2\pi$.

This equation is the same as Eq. (29) for the stable spinning solution studied in model 1. The critical point is given by

$$J_m^{(c)} = J_1^{(c)} = \frac{4}{\pi g(\omega_0)} = 2J_0^{(c)}. \quad (47)$$

That is, the critical point for S_m is the same as the one for the S solution in model 1. The synchronized solution is expressed as

$$\begin{aligned}\alpha_\theta &= \Theta'_c \mp m\theta,\\ \phi^*_\theta &= \omega_0 t + \psi^*_\theta + \alpha_\theta\\ &= \omega_0 t + \sin^{-1}\left(\frac{\omega_\theta - \omega_0}{J_m R_{mc}}\right) + \Theta'_c \mp m\theta. \quad (48)\end{aligned}$$

The entrained phase of the solution changes by $\pm 2\pi m$ when the location θ changes by 2π; that is, its rotation number is $\pm m$.

B. Pendulum solution

Here, we assume $R_m R_n \neq 0$. Moreover, for simplicity, we assume $n \neq 3m$. Accordingly, the conditions on the stable Pn solution are

$$\sin(\Theta_{mc} - \Theta_{ms}) = 0, \quad \sin(\Theta_{nc} - \Theta_{ns}) = 0,$$
$$\cos(\Theta_{nc} - \Theta_{ms}) = 0. \quad (49)$$

Here, we define

$$\bar{\theta}_k = \varphi_k e^{i(\Theta_{kc} - \Theta_{ks})} = \varphi_k \cos(\Theta_{kc} - \Theta_{ks}),$$
$$\tilde{\theta} = \bar{\theta}_n - \bar{\theta}_m, \quad \theta' = \theta - \bar{\theta}_m,$$

from which we obtain

$$\begin{aligned}A_\theta &= A_{\theta' + \bar{\theta}_m}\\ &= \sqrt{[J_m R_m \cos(m\theta')]^2 + [J_n R_n \cos\{n(\theta' - \tilde{\theta})\}]^2}. \quad (50)\end{aligned}$$

By changing the variable from θ to θ', the SCEs become

$$1 = \frac{J_m}{\pi}\int_0^{\pi/2} d\psi \int_0^{2\pi} d\theta' g(\omega_0 + A_{\theta'+\bar{\theta}_m}\sin\psi) \times \cos^2\psi \cos^2(m\theta'), \quad (51)$$

$$1 = \frac{J_n}{\pi}\int_0^{\pi/2} d\psi \int_0^{2\pi} d\theta' g(\omega_0 + A_{\theta'+\bar{\theta}_m}\sin\psi) \times \cos^2\psi \cos^2\{n(\theta' - \tilde{\theta})\}. \quad (52)$$

Furthermore, we derive the condition

$$\langle \sin\{2n(\theta' - \tilde{\theta})\}\rangle = 0. \quad (53)$$

The sufficient condition for this is $\cos(2n\tilde{\theta}) = 0$ or $\sin(2n\tilde{\theta}) = 0$, and it determines the value of $\tilde{\theta}$. Setting $\bar{\alpha}_\theta = \alpha_\theta - \Theta_{ms}$, we obtain

$$A_\theta \cos\bar{\alpha}_\theta = J_m R_m \cos(\Theta_{mc} - \Theta_{ms})\cos(m\theta'), \quad (54)$$

$$A_\theta \sin\bar{\alpha}_\theta = J_n R_n \sin(\Theta_{nc} - \Theta_{ms})\cos\{n(\theta' - \tilde{\theta})\}. \quad (55)$$

Thus,

$$\phi^*_\theta = \omega_0 t + \sin^{-1}\left(\frac{\omega_\theta - \omega_0}{A_\theta}\right) + \bar{\alpha}_\theta + \Theta'_{ms}. \quad (56)$$

This formula indicates that the rotation number can take on values of $0, \pm 1, \ldots, \pm m$.

C. Numerical results

We performed numerical simulations in which we used a Gaussian distribution for $g(\omega)$. We set the mean to be 0, i.e., $\omega_0 = 0$ and standard deviation σ. We studied the case of $m = 1$ and $n = 2$. Figure 8 plots the time series of the amplitudes of the complex order parameters for S_1, S_2, and Pn. The trajectories of the amplitudes of the complex order parameters for S_1 and S_2 converge, but those for Pn fluctuate. Figure 9 shows the time series of the phases of the complex order parameters and $4\tilde{\theta}$. Moreover, Figs. 10 and 11, respectively, display the J_2 dependence of the order parameters for $J_1 = J_2$ and the θ dependencies of the entrained phases ϕ^*_θ. The rotation numbers for the S_1, S_2, and Pn solutions are −1, 2, and 0, respectively. The theoretical and numerical results agree quite well. Figure 12 shows the resultant frequency distribution $G(\tilde{\omega})$ of the S_1 and S_2 solutions, and the location-dependent resultant frequency distribution $G(\tilde{\omega},\theta)$ for different θ of the Pn solution. Agreement between numerical and theoretical results is excellent for the S_1 and S_2 solutions. However, it is not close for the Pn solution. This is because the trajectories of R_1 and R_2 for the Pn solution fluctuate, as shown in Fig. 8(c). As can be seen from Fig. 9, $\Theta_{1c} - \Theta_{1s} = -\pi, \Theta_{2c} - \Theta_{2s} = 0, \Theta_{2c} - \Theta_{1s} = -\pi/2$. Thus, $\bar{\theta}_1 = -\varphi_1$ and $\bar{\theta}_2 = \varphi_2$. Therefore, $0 \leqslant 4\tilde{\theta} \leqslant 3\pi$. Accordingly,

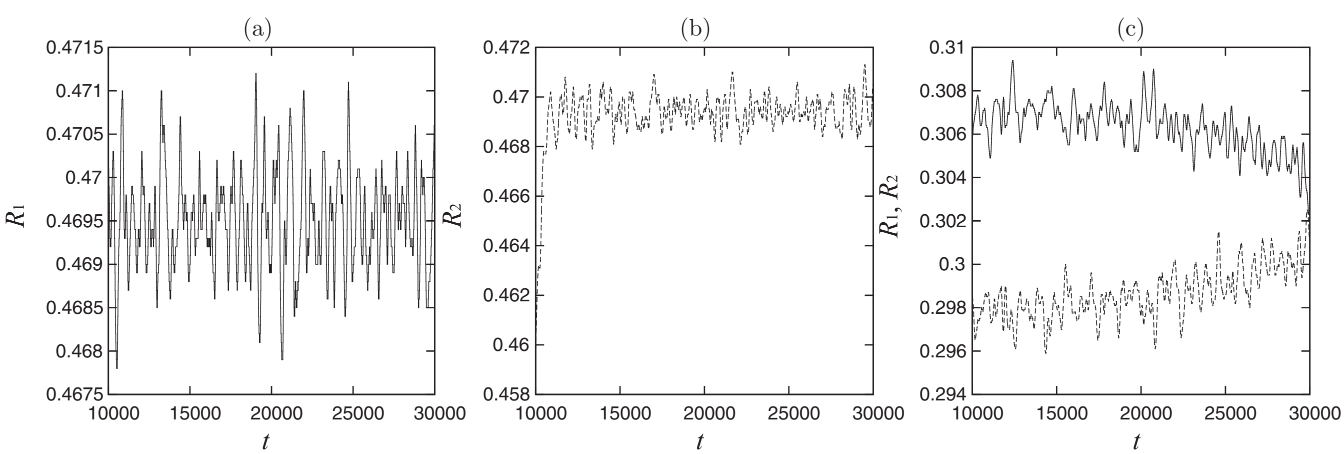

FIG. 8. Trajectories of R_1 and R_2. $J_1 = J_2 = 1.2J_{1,c}$. $N = 200\,000$. Solid curve: R_1, dashed curve: R_2. (a) S_1 solution. (b) S_2 solution. (c) Pn solution.

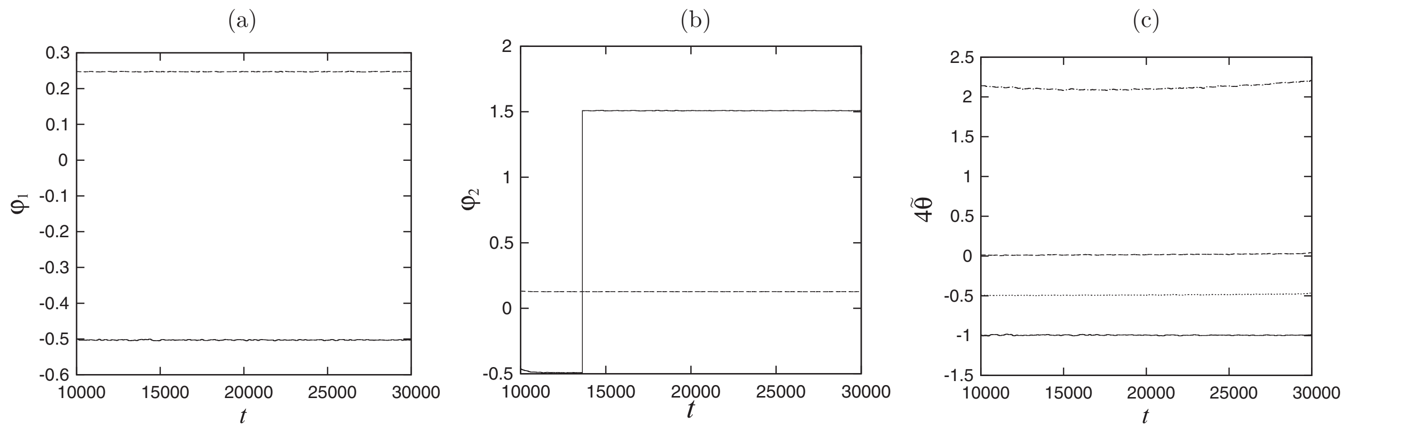

FIG. 9. Trajectories of φ's and $4\tilde{\theta}$. $J_1 = J_2 = 1.2J_{1,c}$. $N = 200\,000$. (a) S_1 solution. Solid curve: $\Theta_{1c} - \Theta_{1s}$, dashed curve: φ_1. (b) S_2 solution. Solid curve: $\Theta_{2c} - \Theta_{2s}$, dashed curve: φ_2. (c) Pn solution. Solid curve: $\Theta_{1c} - \Theta_{1s}$, dashed curve: $\Theta_{2c} - \Theta_{2s}$, dotted curve: $\Theta_{2c} - \Theta_{1s}$, dashed dotted curve: $4\tilde{\theta}$.

the condition $\cos(4\tilde{\theta}) = 0$ implies $4\tilde{\theta} = \frac{\pi}{2}, \frac{3\pi}{2}, \frac{5\pi}{2}$. The other condition $\sin(4\tilde{\theta}) = 0$ implies $4\tilde{\theta} = 0,\pi,2\pi,3\pi$. However, numerical results show that $4\tilde{\theta} \simeq 2.2\pi$ [Fig. 9(c)]. This is the cause of the discrepancy between the theoretical and numerical results for $G(\tilde{\omega},\theta)$.

VIII. SUMMARY AND DISCUSSION

We studied phase oscillator networks on a circle with two types of interaction (models 1 and 2).

Model 1 is the Mexican-hat interaction. The interaction is composed of two terms, one of which is a uniform interaction with strength J_0, and the other is a sinusoidal interaction with respect to the location θ of oscillators with strength J_1. If $J_1 = 0$, the present model reduces to the Kuramoto model. To obtain self-consistent equations, information about the differences between the phases of the complex order parameters is necessary. Previously, for this purpose, we studied the classical XY model to which the phase oscillator network reduces when all oscillators have the same natural frequency [29,30]. The relevant order parameters are the same in the oscillator network and the XY model. The order parameters that characterize the solutions are R and R_1. The saddle point equations (SPEs) for the XY model were obtained and the differences between the phases of the complex order parameters were determined analytically [30]. So far, we have used information on the phases of the complex order parameters in the XY model to solve the SCEs for the phase oscillator network. Recently, we succeeded in deriving auxiliary equations that determine the phases of the order parameters for the phase oscillator network. The auxiliary equations turned out to be the same as the SPEs for the phases of the complex order parameters in the XY model [26]. In this paper, we gave detailed derivations of the relevant equations and quantities. We derived two auxiliary equations by expressing the order parameters in terms of the number density of the oscillators. We used them to analytically determine the phases of the order parameters, derived self-consistent equations for their amplitudes, and obtained three nontrivial solutions that are characterized by the order parameters and the rotation numbers of the synchronized oscillators X^*_θ. We drew the phase diagram by using formulas for the phase boundaries derived using the unstable Pn solution. Furthermore, we found that the disappearance of coexistent regions between the U and S solutions and between the Pn and S solutions is due to annihilation of the unstable Pn and stable S solutions, and that of the unstable and stable Pn solutions. This type of transition does not exist in the Kuramoto model. We also analytically obtained the location-dependent distribution of the resultant frequencies and entrained phases and validated the theoretical results by simulation, except for the chaotic behavior of the desynchronized oscillators. This chaotic behavior is quite reasonable because quasiperiodic motion with more than two dimensions generically becomes chaotic through perturbation

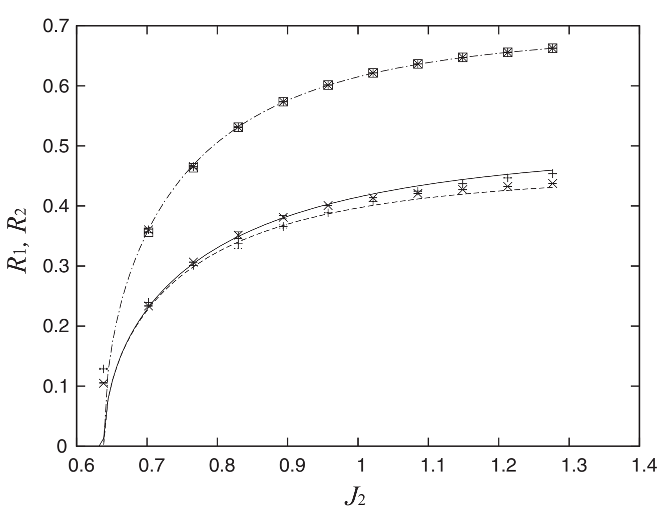

FIG. 10. J_2 dependence of R_1,R_2. $\sigma = 0.2$. $J_1 = J_2$. $J_2/J_{2,c}i$, $i = 0.8,0.2,\ldots,2.0$. $\omega_0 = 0$. Curves: theory. Symbols: simulation. $N = 10\,000$. The sample average was taken over 40 initial configurations. Solid curve and $+$: R_1 of Pn, dashed curve and $\times$: R_2 of Pn, dashed-dotted curve: R_1 of S_1 and R_2 of S_2, $*$: R_1 of S_1, square: R_2 of S_2. Vertical lines are error bars. The error bars on almost all of the data are too small to see.

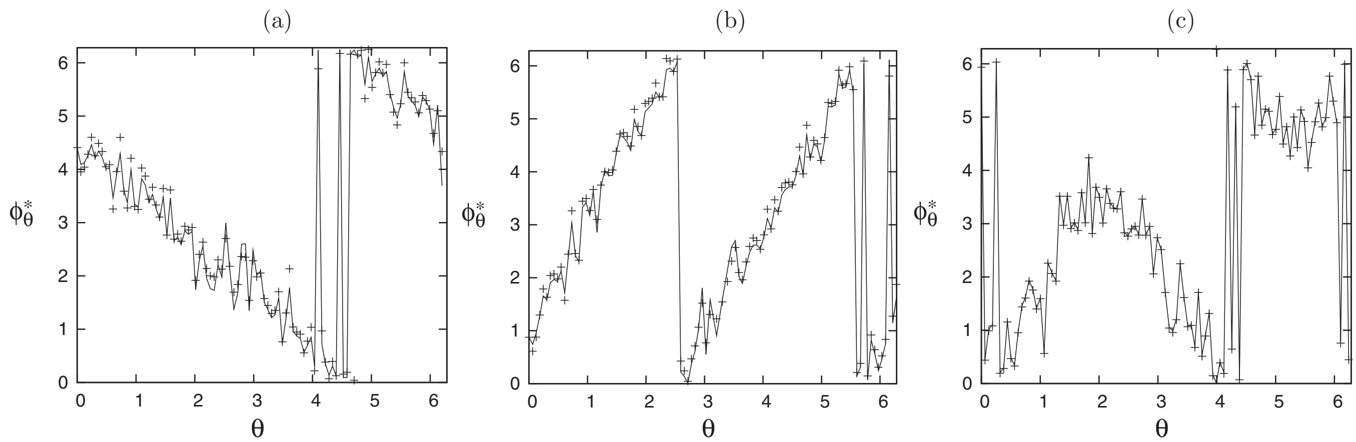

FIG. 11. θ dependencies of entrained phases ϕ^*_θ. Line plots: theory; +: simulation. The theoretical values are calculated using Eq. (56) with $\omega_0 = 0$, and these values are connected by straight lines so that it is easier to compare them with the numerical results. Only 1% of the entrained phases are depicted. $J_1 = J_2 = 1.8J_{1,c}, \sigma = 0.2$. Simulation: $N = 10\,000$. (a) S_1 solution. (b) S_2 solution. (c) Pn solution.

[28]. Our numerical results suggest that the system behaves quasiperiodically as N goes to infinity.

Model 2 is an interaction including the mth and nth Fourier components, where $m < n$. We found spinning solutions, S_m

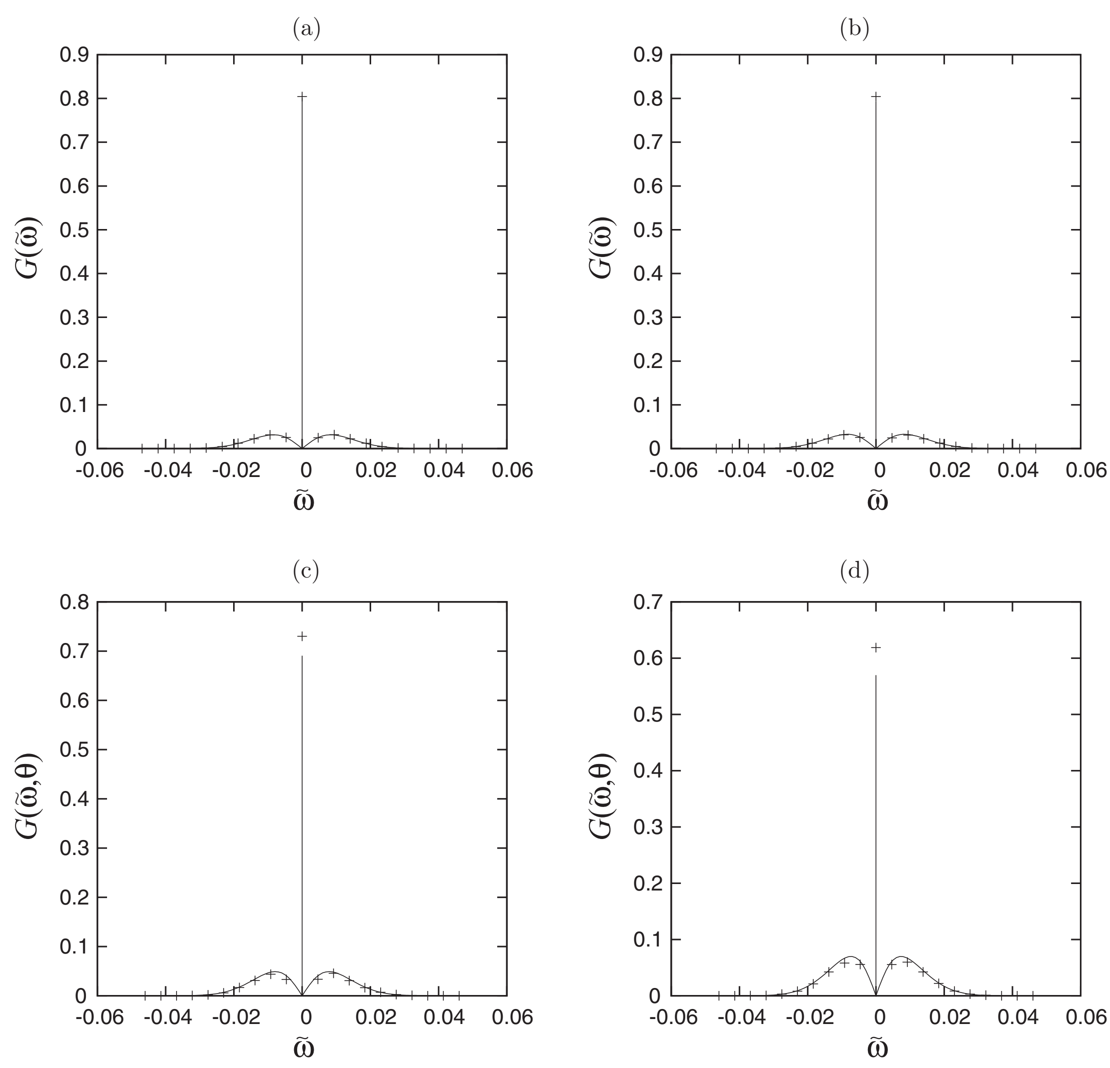

FIG. 12. Theoretical and simulated results for the distribution of the resultant frequencies. $G(\tilde{\omega})$ for the S_1 and S_2 solutions and $G(\tilde{\omega},\theta)$ for the Pn solution. Curve: theory, +: simulation ($N = 200\,000, \sigma = 0.01, J_1 = J_2 = 1.2J_{1,c}$). (a) S_1 solution, (b) S_2 solution, (c) $\theta = 0.05 \times 2\pi$ for Pn solution, (d) $\theta = 0.25 \times 2\pi$ for Pn solution.

and S_n, and a pendulum solution. The critical points for the S_m and S_n solutions are the same as those for the S solution in model 1. In S_m (S_n), the phase of the entrained oscillators changes by $\pm 2m\pi$ ($\pm 2n\pi$) when the location changes by 2π. That is, the rotation number is $\pm m$ ($\pm n$). On the other hand, in the pendulum solution, the phase of the entrained oscillators fluctuates when location changes by 2π, and the rotation number can take on values of $0, \pm 1, \pm 2, \ldots, \pm m$. We performed a similar analysis to that of model 1 for $m = 1$ and $n = 2$. In the J_1, J_2 space, around the line $J_1 = J_2$, these three solutions coexist for $J_1 > J_{1,c}$ and $J_2 > J_{2,c}$. We conducted a simulation that validated the theoretical results for the J_2 dependencies of R_1 and R_2 and the dependencies of the entrained phases on location. As for the distribution of the resultant frequencies, the agreement between the theoretical and numerical results was excellent for the S_1 and S_2 solutions. However, theoretical and numerical results for the location-dependent distribution of the resultant frequencies did not agree very well for the Pn solution. This is because the trajectories of R_1 and R_2 for the Pn solution fluctuate, and the numerical value of $\tilde{\theta}$ deviates from the theoretical prediction. The reason for this deviation seems to be that the desynchronized oscillators behave more chaotically in the Pn solution than in the S_1 and S_2 solutions.

How the existing phases and phase transitions depend on the type of interaction is an interesting question. The present method is applicable to phase oscillator networks not only on a circle but also in general spaces. For example, we have started to study an oscillator network and XY model in which the interaction is like that of associative memory, and we have found that there are different phases and phase transitions from those in the Mexican-hat interaction.

ACKNOWLEDGMENT

We are grateful to Chie Izumi for performing numerical simulations of model 2 in the early stage of the present work.

APPENDIX A: DERIVATION OF AUXILIARY EQUATIONS AND SCEs, AND SOLUTIONS OF AUXILIARY EQUATIONS

The total number density of oscillators with phase ψ at location θ, $n(\theta,\psi)$, is $n(\theta,\psi) = n_s(\theta,\psi) + n_{\rm ds}(\theta,\psi)$. From Eq. (15), since $n_{\rm ds}(\theta,\psi+\pi) = n_{\rm ds}(\theta,\psi)$, $\int_0^{2\pi} n_{\rm ds}(\theta,\psi) e^{i\psi} d\psi = 0$ follows. Thus, only synchronized oscillators contribute to the order parameters:

$$Re^{i\Theta} = \int_{-\pi}^{\pi} d\psi\, n_s(\psi) e^{i\psi + i\alpha_\theta}, \qquad \text{(A1)}$$

$$R_c e^{i\Theta_c} = \int_{-\pi}^{\pi} d\psi \frac{1}{2\pi} \int_0^{2\pi} d\theta\, n_s(\theta,\psi) \cos\theta e^{i\psi + i\alpha_\theta}, \qquad \text{(A2)}$$

$$R_s e^{i\Theta_s} = \int_{-\pi}^{\pi} d\psi \frac{1}{2\pi} \int_0^{2\pi} d\theta\, n_s(\theta,\psi) \sin\theta e^{i\psi + i\alpha_\theta}, \qquad \text{(A3)}$$

where

$$n_s(\psi) = \frac{1}{2\pi} \int_0^{2\pi} d\theta\, n_s(\theta,\psi).$$

By substituting the expression of $n_s(\theta,\psi)$ into Eq. (A1), we obtain the following equations:

$$R = \frac{1}{\pi} \int_0^{\pi/2} d\psi \int_0^{2\pi} d\theta\, g(\omega_0 + A_\theta \sin\psi) \cos^2\psi \times \{J_0 R + J_1 (R_c \cos\theta e^{i(\Theta_c - \Theta)} + R_s \sin\theta e^{i(\Theta_s - \Theta)})\}. \qquad \text{(A4)}$$

A_θ is expressed as

$$A_\theta^2 = (J_0 R)^2 + J_1^2 \{(R_c \cos\theta)^2 + (R_s \sin\theta)^2 + 2 R_c R_s \cos(\Theta_c - \Theta_s) \sin\theta \cos\theta\} + 2 J_0 J_1 R \{R_c \cos(\Theta_c - \Theta) \cos\theta + R_s \cos(\Theta_s - \Theta) \sin\theta\}.$$

We introduce the following notation:

$$\langle B \rangle \equiv \frac{1}{Z} \int_0^{\pi/2} d\psi \int_0^{2\pi} d\theta g(\omega_0 + A_\theta \sin\psi) \cos^2\psi\, B, \qquad \text{(A5)}$$

$$Z \equiv \int_0^{\pi/2} d\psi \int_0^{2\pi} d\theta g(\omega_0 + A_\theta \sin\psi) \cos^2\psi. \qquad \text{(A6)}$$

Equation (A4) can be rewritten as

$$R = (J_0 R + J_1 \{R_c e^{i(\Theta_c - \Theta)} \langle\cos\theta\rangle + R_s e^{i(\Theta_s - \Theta)} \langle\sin\theta\rangle\}) Z. \qquad \text{(A7)}$$

Similarly, Eqs. (A2), and (A3) can be rewritten as

$$R_c = (J_0 R e^{-i(\Theta_c - \Theta)} \langle\cos\theta\rangle + J_1 \{R_c \langle\cos^2\theta\rangle + R_s e^{-i(\Theta_c - \Theta_s)} \langle\sin\theta\cos\theta\rangle\}) Z, \qquad \text{(A8)}$$

$$R_s = (J_0 R e^{-i(\Theta_s - \Theta)} \langle\sin\theta\rangle + J_1 \{R_c e^{i(\Theta_c - \Theta_s)} \langle\sin\theta\cos\theta\rangle + R_s \langle\sin^2\theta\rangle\}) Z. \qquad \text{(A9)}$$

The real parts of Eqs. (A7), (A8), and (A9) give the SCEs for R, R_c, and R_s,

$$R = (J_0 R + J_1 \{R_c \langle\cos\theta\rangle \cos(\Theta_c - \Theta) + R_s \langle\sin\theta\rangle \cos(\Theta_s - \Theta)\}) Z, \qquad \text{(A10)}$$

$$R_c = (J_0 R \langle\cos\theta\rangle \cos(\Theta_c - \Theta) + J_1 \{R_c \langle\cos^2\theta\rangle + R_s \langle\sin\theta\cos\theta\rangle \cos(\Theta_c - \Theta_s)\}) Z, \qquad \text{(A11)}$$

$$R_s = (J_0 R \langle\sin\theta\rangle \cos(\Theta_s - \Theta) + J_1 \{R_c \langle\sin\theta\cos\theta\rangle \times \cos(\Theta_c - \Theta_s) + R_s \langle\sin^2\theta\rangle\}) Z. \qquad \text{(A12)}$$

The imaginary parts of Eqs. (A7), (A8), and (A9) give three equations,

$$R_c \langle\cos\theta\rangle \sin(\Theta_c - \Theta) + R_s \langle\sin\theta\rangle \sin(\Theta_s - \Theta) = 0, \qquad \text{(A13)}$$

$$J_0 R \langle\cos\theta\rangle \sin(\Theta_c - \Theta) + J_1 R_s \langle\sin\theta\cos\theta\rangle \sin(\Theta_c - \Theta_s) = 0, \qquad \text{(A14)}$$

$$J_0 R \langle\sin\theta\rangle \sin(\Theta_s - \Theta) - J_1 R_c \langle\sin\theta\cos\theta\rangle \sin(\Theta_c - \Theta_s) = 0. \qquad \text{(A15)}$$

Two of Eqs. (A13), (A14), and (A15) are independent. These auxiliary equations completely determine the phases of the order parameters.

Now, let us solve the auxiliary equations. We will concentrate on the solutions that are relevant to the phase transitions. First, we solve the case of $R = 0$ and $R_1 = \sqrt{R_c^2 + R_s^2} \neq 0$ and derive the phases of the order parameters for the stable S solution.

Case of $R = 0, R_1 \neq 0$. Since A_θ does not have $\cos\theta$ and $\sin\theta$ terms, $\langle\cos\theta\rangle = \langle\sin\theta\rangle = 0$ follows. Thus, from Eqs. (A14) and (A15), we obtain

$$J_1 R_s \langle\sin\theta\cos\theta\rangle \sin(\Theta_c - \Theta_s) = 0, \tag{A16}$$

$$J_1 R_c \langle\sin\theta\cos\theta\rangle \sin(\Theta_c - \Theta_s) = 0. \tag{A17}$$

Therefore, we have

$$\langle\sin\theta\cos\theta\rangle \sin(\Theta_c - \Theta_s) = 0.$$

The case of $\sin(\Theta_c - \Theta_s) = 0$ gives an irrelevant solution, so we will omit discussion of this case.

Now let us study the case $\langle\sin\theta\cos\theta\rangle = 0$. Here, the Fourier expansion of the integrand should not contain the Fourier component $\sin\theta\cos\theta$. Therefore, the coefficient of $\sin\theta\cos\theta$ in A_θ should be 0, that is, $R_c R_s \cos(\Theta_c - \Theta_s) = 0$. Thus, $\cos(\Theta_c - \Theta_s) = 0$, or $R_c = 0$, or $R_s = 0$. $R_c = 0$ or $R_s = 0$ gives irrelevant solutions, and the relevant solution is when $\cos(\Theta_c - \Theta_s) = 0$, that is, $\Theta_c - \Theta_s = \pm\frac{\pi}{2} \pmod{2\pi}$. Hereafter, we omit "(mod 2π)" for simplicity. Numerical results show that this case corresponds to the stable S solution.

Next, we solve the case of $R \neq 0, R_c \neq 0, R_s \neq 0$ and derive the phases of the order parameters for the Pn solutions.

Case of $R \neq 0, R_c \neq 0, R_s \neq 0$. Using Eq. (A14) and $\Theta_s - \Theta = (\Theta_c - \Theta) - (\Theta_c - \Theta_s)$ and multiplying Eq. (A15) by $\langle\cos\theta\rangle$, we obtain

$$\begin{aligned}\sin(\Theta_c - \Theta_s)[&J_1 R_s\langle\sin\theta\cos\theta\rangle\langle\sin\theta\rangle\cos(\Theta_c - \Theta_s)\\ &+ \langle\cos\theta\rangle\{J_0 R\langle\sin\theta\rangle\cos(\Theta_c - \Theta)\\ &+ J_1 R_c\langle\sin\theta\cos\theta\rangle\}] = 0.\end{aligned} \tag{A18}$$

Case 1 $\sin(\Theta_c - \Theta_s) = 0$, that is, $\Theta_c - \Theta_s = \{0,\pi\}$.
From Eq. (A14), we obtain

$$J_0 R\langle\cos\theta\rangle \sin(\Theta_c - \Theta) = 0.$$

Thus, $\Theta_c - \Theta = \{0,\pi\}$ or $\langle\cos\theta\rangle = 0$ follows. The relevant solution is obtained from the case $\langle\cos\theta\rangle = 0$. In this case, A_θ should not contain any $\cos\theta$ term, that is, $RR_c\cos(\Theta_c - \Theta)\langle\sin\theta\cos\theta\rangle = 0$. Therefore, $\cos(\Theta_c - \Theta) = 0$, i.e., $\Theta_c - \Theta = \pm\frac{\pi}{2}$. Since $\Theta_s - \Theta = (\Theta_c - \Theta) - (\Theta_c - \Theta_s) = \pm\frac{\pi}{2}$, we obtain

$$\{\Theta_c - \Theta, \Theta_s - \Theta\} = \left\{\pm\frac{\pi}{2}, \pm\frac{\pi}{2}\right\}.$$

Numerical results show that this is the stable Pn solution.

Using Eq. (A13) and $\Theta_c - \Theta_s = (\Theta_c - \Theta) - (\Theta_s - \Theta)$ and multiplying Eq. (A14) by $\langle\sin\theta\rangle$, we obtain

$$\begin{aligned}\sin(\Theta_c - \Theta)[&\langle\sin\theta\rangle\{J_0 R\langle\cos\theta\rangle\\ &+ J_1 R_s\langle\sin\theta\cos\theta\rangle\cos(\Theta_s - \Theta)\}\\ &+ J_1 R_c\langle\sin\theta\cos\theta\rangle\langle\cos\theta\rangle\cos(\Theta_c - \Theta)] = 0.\end{aligned} \tag{A19}$$

Case 2 $\sin(\Theta_c - \Theta) = 0$, that is, $\Theta_c - \Theta = \{0,\pi\}$.
From Eq. (A13), $R_s\langle\sin\theta\rangle\sin(\Theta_s - \Theta) = 0$. Thus, $\Theta_s - \Theta = \{0,\pi\}$, or $\langle\sin\theta\rangle = 0$. The relevant solution is obtained from $\langle\sin\theta\rangle = 0$. In this case, $RR_s\cos(\Theta_s - \Theta)$ should be 0. Therefore, $\cos(\Theta_s - \Theta) = 0$, that is, $\Theta_s - \Theta = \pm\frac{\pi}{2}$. Thus, we obtain

$$\{\Theta_c - \Theta, \Theta_s - \Theta\} = \left\{0 \text{ or } \pi, \pm\frac{\pi}{2}\right\}.$$

It turns out that this Pn solution is unstable.

Using Eq. (A13) and $\Theta_c - \Theta_s = (\Theta_c - \Theta) - (\Theta_s - \Theta)$ and multiplying Eq. (A15) by $\langle\cos\theta\rangle$, we obtain

$$\begin{aligned}\sin(\Theta_s - \Theta)[&\langle\cos\theta\rangle\{J_0 R\langle\sin\theta\rangle\\ &+ J_1 R_c\langle\sin\theta\cos\theta\rangle\cos(\Theta_c - \Theta)\}\\ &+ J_1 R_s\langle\sin\theta\cos\theta\rangle\langle\sin\theta\rangle\cos(\Theta_s - \Theta)] = 0.\end{aligned} \tag{A20}$$

Case 3 $\sin(\Theta_s - \Theta) = 0$*, that is,* $\Theta_s - \Theta = \{0,\pi\}$.
In this case, from Eq. (A13), we have

$$R_c\langle\cos\theta\rangle\sin(\Theta_c - \Theta) = 0.$$

It follows that $\Theta_c - \Theta = \{0,\pi\}$, or $\langle\cos\theta\rangle = 0$.

Case 3-1. $\sin(\Theta_c - \Theta) = 0$.

Moreover, it follows that $\{\Theta_c - \Theta, \Theta_s - \Theta\} = \{0 \text{ or } \pi, 0 \text{ or } \pi\}$. These solutions are unstable and irrelevant.

Case 3-2. $\langle\cos\theta\rangle = 0$.

In this case, $RR_c\cos(\Theta_c - \Theta)$ should be 0. Thus, $\cos(\Theta_c - \Theta) = 0$, and $\Theta_c - \Theta = \pm\frac{\pi}{2}$. Therefore, we have $\{\Theta_c - \Theta, \Theta_s - \Theta\} = \{\pm\frac{\pi}{2}, 0 \text{ or } \pi\}$. These solutions are unstable.

Other cases.

The other conditions for (A18), (A19), and (A20) are

$$\begin{aligned}J_1 R_s&\langle\sin\theta\cos\theta\rangle\langle\sin\theta\rangle\cos(\Theta_c - \Theta_s)\\ &+ \langle\cos\theta\rangle\{J_0 R\langle\sin\theta\rangle\cos(\Theta_c - \Theta)\\ &+ J_1 R_c\langle\sin\theta\cos\theta\rangle\} = 0,\end{aligned} \tag{A21}$$

$$\begin{aligned}\langle\sin\theta\rangle\{&J_0 R\langle\cos\theta\rangle + J_1 R_s\langle\sin\theta\cos\theta\rangle\cos(\Theta_s - \Theta)\}\\ &+ J_1 R_c\langle\sin\theta\cos\theta\rangle\langle\cos\theta\rangle\cos(\Theta_c - \Theta) = 0,\end{aligned} \tag{A22}$$

$$\begin{aligned}\langle\cos\theta\rangle\{&J_0 R\langle\sin\theta\rangle + J_1 R_c\langle\sin\theta\cos\theta\rangle\cos(\Theta_c - \Theta)\}\\ &+ J_1 R_s\langle\sin\theta\cos\theta\rangle\langle\sin\theta\rangle\cos(\Theta_s - \Theta) = 0.\end{aligned} \tag{A23}$$

Since R, R_c, and R_s are continuous functions with respect to the parameters J_0 and J_1, the conditions under which the above equalities hold are that the coefficients of R, R_c, R_s are 0. The conditions for $\langle\cos\theta\rangle = 0$ and for $\cos(\Theta_c - \Theta) = 0$ are the same, and $\Theta_c - \Theta = \pm\frac{\pi}{2}$. Similarly, the condition for $\langle\sin\theta\rangle = 0$ and for $\cos(\Theta_s - \Theta) = 0$ is $\Theta_s - \Theta = \pm\frac{\pi}{2}$, and the condition for $\langle\sin\theta\cos\theta\rangle = 0$ and for $\cos(\Theta_c - \Theta_s) = 0$ is $\Theta_c - \Theta_s = \pm\frac{\pi}{2}$. The combination of phases of the order parameters is the same as that in cases 1 to 3.

APPENDIX B: DERIVATION OF CONCRETE SCEs AND RELEVANT QUANTITIES FOR EACH PHASE

1. Stable uniform solution

This is the case of $R > 0$ and $R_1 = 0$. This is merely the solution of the Kuramoto model. Since $R_1 = 0$, we have

$$A_\theta e^{i\alpha_\theta} = J_0 R e^{i\Theta}, \quad A_\theta = J_0 R, \quad \alpha_\theta = \Theta' = \text{const}.$$

Therefore, the entrained phase ϕ_θ^* is expressed as

$$\phi_\theta^* = \omega_0 t + \Theta' + \sin^{-1}\left(\frac{\omega_\theta - \omega_0}{J_0 R}\right).$$

Note that $\Theta' = \Theta - \omega_0 t$ is used in the expressions of α_θ ad ϕ_θ^*. The SCE is

$$R = 2J_0 R \int_0^{\pi/2} d\psi\, g(\omega_0 + J_0 R \sin\psi)\cos^2\psi. \quad \text{(B1)}$$

The phase transition point from the P phase to the U phase is

$$J_{0,c} = \frac{2}{\pi g(\omega_0)}. \quad \text{(B2)}$$

2. Stable S solution

For the stable S solution, $R = 0$, $\langle\cos\theta\rangle = \langle\sin\theta\rangle = 0$, and $\Theta_c - \Theta_s = \pm\frac{\pi}{2}$ (see Appendix A). In this case, A_θ is expressed as $A_\theta = J_1\sqrt{(R_c\cos\theta)^2 + (R_s\sin\theta)^2}$. From Eqs. (A11) and (A12), we have

$$R_c = J_1 R_c \langle\cos^2\theta\rangle Z, \quad R_s = J_1 R_s \langle\sin^2\theta\rangle Z.$$

If $R_c R_s \neq 0$, then $\langle\cos^2\theta\rangle = \langle\sin^2\theta\rangle$ holds. $R_c = R_s = \frac{R_1}{\sqrt{2}}$ follows from this. Accordingly, $A_\theta = J_1 R_c$, and the SCE becomes

$$R_c = J_1 R_c \int_0^{\pi/2} d\psi\, g(\omega_0 + J_1 R_c \sin\psi)\cos^2\psi. \quad \text{(B3)}$$

The phase transition point from the P phase to the S phase and the order parameter R_1 near to the transition point are given by

$$J_{1,c} = \frac{4}{g(\omega_0)\pi} = 2J_{0,c},$$
$$R_1 \simeq \frac{4}{J_{1,c}^2}\sqrt{\frac{2(J_1 - J_{1,c})}{\pi|g''(\omega_0)|}} \propto \sqrt{J_1 - J_{1,c}}.$$

When $g(\omega)$ is a Gaussian distribution with mean ω_0 and standard deviation σ, $J_{0,c}$ and $J_{1,c}$ are given by

$$J_{0,c} = 2\sqrt{\frac{2}{\pi}}\sigma, \quad J_{1,c} = 4\sqrt{\frac{2}{\pi}}\sigma = 2J_{0,c}. \quad \text{(B4)}$$

Let us study the entrained phase $\phi_\theta^* = \omega_0 t + \psi_\theta^* + \alpha_\theta$. Since $\Theta_c - \Theta_s = \pm\frac{\pi}{2}$, $\Theta_s = \Theta_c - (\Theta_c - \Theta_s) = \Theta_c \mp \frac{\pi}{2}$. From Eq. (8), we have

$$A_\theta e^{i\alpha_\theta} = J_1 R_c e^{i\Theta_c}(\cos\theta + \sin\theta e^{\mp i\frac{\pi}{2}}) = J_1 R_c e^{i(\Theta_c \mp \theta)}. \quad \text{(B5)}$$

Therefore, $A_\theta = J_1 R_c$ and $\alpha_\theta = \Theta_c' \mp \theta$. Accordingly, the entrained phase ϕ_θ^* is

$$\phi_\theta^* = \omega_0 t + \psi_\theta^* + \alpha_\theta$$
$$= \omega_0 t + \sin^{-1}\left(\frac{\omega_\theta - \omega_0}{J_1 R_c}\right) + \Theta_c' \mp \theta. \quad \text{(B6)}$$

Thus, the entrained phase ϕ_θ^* linearly depends on the location θ.

3. Stable Pn solution

Since $\{\Theta_c - \Theta, \Theta_s - \Theta\} = \{\pm\frac{\pi}{2}, \pm\frac{\pi}{2}\}$, by using $\sin(\Theta_c - \Theta) = \pm 1$, $\cos(\Theta_c - \Theta) = 0$, $\cos(\Theta_c - \Theta_s) = \pm 1$, and $\sin(\Theta_c - \Theta_s) = 0$, Eq. (8) reduces to

$$A_\theta e^{i\alpha_\theta} = J_0 R e^{i[\Theta_c - (\Theta_c - \Theta)]}$$
$$+ J_1 R_1 e^{i\Theta_c}\cos\{\theta - \varphi\cos(\Theta_c - \Theta_s)\}, \quad \text{(B7)}$$

where we have defined

$$R_c = R_1\cos\varphi, \quad R_s = R_1\sin\varphi.$$

Therefore, setting $\bar{\alpha}_\theta = \alpha_\theta - \Theta_c$, we have

$$A_\theta \sin\bar{\alpha}_\theta = -J_0 R \sin(\Theta_c - \Theta),$$
$$A_\theta \cos\bar{\alpha}_\theta = J_1 R_1 \cos\{\theta - \varphi\cos(\Theta_c - \Theta_s)\}, \quad \text{(B8)}$$
$$A_\theta = \sqrt{(J_0 R)^2 + (J_1 R_1)^2\cos^2\{\theta - \varphi\cos(\Theta_c - \Theta_s)\}}.$$

Equations (A10), (A11), and (A12) become

$$R = J_0 R Z, \quad \text{(B9)}$$

$$R_c = J_1 R_1 Z\langle\cos^2\{\theta - \varphi\cos(\Theta_c - \Theta_s)\}\rangle\cos\varphi, \quad \text{(B10)}$$

$$R_s = J_1 R_1 Z\langle\cos^2\{\theta - \varphi\cos(\Theta_c - \Theta_s)\}\rangle\sin\varphi. \quad \text{(B11)}$$

By transforming θ into $\theta' = \theta - \varphi\cos(\Theta_c - \Theta_s)$ and since $A_{\theta' + \varphi\cos(\Theta_c - \Theta_s)}$ is periodic with period π and an even function of θ', we obtain the following SCEs:

$$R = \frac{4J_0 R}{\pi}\int_0^{\pi/2} d\psi \int_0^{\pi/2} d\theta'$$
$$\times g(\omega_0 + A_{\theta' + \varphi\cos(\Theta_c - \Theta_s)}\sin\psi)\cos^2\psi, \quad \text{(B12)}$$

$$R_1 = \frac{4J_1 R_1}{\pi}\int_0^{\pi/2} d\psi \int_0^{\pi/2} d\theta'$$
$$\times g(\omega_0 + A_{\theta' + \varphi\cos(\Theta_c - \Theta_s)}\sin\psi)\cos^2\psi\cos^2\theta', \quad \text{(B13)}$$

$$A_{\theta' + \varphi\cos(\Theta_c - \Theta_s)} = \sqrt{(J_0 R)^2 + (J_1 R_1)^2\cos^2\theta'}. \quad \text{(B14)}$$

In this solution, we have

$$\phi_\theta^* = \omega_0 t + \alpha_\theta + \sin^{-1}\left(\frac{\omega_\theta - \omega_0}{A_\theta}\right) = \omega_0 t + \bar{\alpha}_\theta + \Theta_c'$$
$$+ \sin^{-1}\left(\frac{\omega_\theta - \omega_0}{A_\theta}\right), \quad \text{(B15)}$$

where θ is the original coordinate and A_θ is given by Eq. (B8).

4. Unstable Pn solution

Since $\{\Theta_c - \Theta, \Theta_s - \Theta\} = \{0 \text{ or } \pi, \pm\frac{\pi}{2}\}$, then $\sin(\Theta_c - \Theta) = 0$, $\cos(\Theta_c - \Theta) = \pm 1$, $\sin(\Theta_s - \Theta) = \pm 1$, $\cos(\Theta_s - \Theta) = 0$, $\sin(\Theta_c - \Theta_s) = \pm 1$, and $\cos(\Theta_c - \Theta_s) = 0$. Equation (8) reduces to

$$A_\theta e^{i\alpha_\theta} = e^{i\Theta_c}[J_0 R e^{-i(\Theta_c - \Theta)} + J_1 R_c\cos\theta$$
$$- iJ_1 R_s \sin\theta\sin(\Theta_c - \Theta_s)].$$

Therefore, setting $\bar{\alpha}_\theta = \alpha_\theta - \Theta_c$, we have

$$\begin{aligned} A_\theta \sin\bar{\alpha}_\theta &= -J_1 R_s \sin\theta \sin(\Theta_c - \Theta_s), \\ A_\theta \cos\bar{\alpha}_\theta &= J_0 R \cos(\Theta_c - \Theta) + J_1 R_c \cos\theta, \\ A_\theta &= \sqrt{[J_0 R \cos(\Theta_c - \Theta) + J_1 R_c \cos\theta]^2 + (J_1 R_s \sin\theta)^2} \\ &= \sqrt{[J_0 R + J_1 R_c \cos\{\theta - (\Theta_c - \Theta)\}]^2 + [J_1 R_s \sin\{\theta - (\Theta_c - \Theta)\}]^2}. \end{aligned} \tag{B16}$$

Accordingly, Eqs. (A10), (A11), and (A12) become

$$R = \langle J_0 R + J_1 R_c \cos\{\theta - (\Theta_c - \Theta)\}\rangle Z, \tag{B17}$$

$$R_c = \langle [J_0 R + J_1 R_c \cos\{\theta - (\Theta_c - \Theta)\}] \times \cos\{\theta - (\Theta_c - \Theta)\}\rangle Z, \tag{B18}$$

$$R_s = \langle J_1 R_s \sin^2\{\theta - (\Theta_c - \Theta)\}\rangle Z. \tag{B19}$$

By transforming θ into $\theta' = \theta - (\Theta_c - \Theta)$ and since $A_{\theta'+\Theta_c-\Theta}$ is periodic with period π and an even function of θ', Eqs. (B17), (B18), and (B19) can be expressed as

$$R = \frac{2}{\pi}\int_0^{\pi/2} d\psi \int_0^{\pi} d\theta' g(\omega_0 + A_{\theta'+\Theta_c-\Theta}\sin\psi) \times \cos^2\psi\,(J_0 R + J_1 R_c \cos\theta'), \tag{B20}$$

$$R_c = \frac{2}{\pi}\int_0^{\pi/2} d\psi \int_0^{\pi} d\theta' g(\omega_0 + A_{\theta'+\Theta_c-\Theta}\sin\psi) \times \cos^2\psi\,(J_0 R + J_1 R_c \cos\theta')\cos\theta', \tag{B21}$$

$$R_s = J_1 R_c \frac{2}{\pi}\int_0^{\pi/2} d\psi \int_0^{\pi} d\theta' g(\omega_0 + A_{\theta'+\Theta_c-\Theta}\sin\psi) \times \cos^2\psi\, \sin^2\theta', \tag{B22}$$

where $A_{\theta'+\Theta_c-\Theta} = \sqrt{(J_0 R + J_1 R_c \cos\theta')^2 + (J_1 R_s \sin\theta')^2}$.

APPENDIX C: CONDITION ON THE EXISTENCE OF THE Pn SOLUTION, $J_1 > 2J_0$

Let us consider a bifurcation from a solution with $R > 0$ and $R_1 = 0$ to a solution with $R > 0$ and $R_1 > 0$. Let us define $X(R)$ and $Y(R)$ as follows:

$$X(R) \equiv \frac{2}{\pi}\int_0^{\pi/2} d\psi\, g(\omega_0 + J_0 R\sin\psi)\cos^2\psi, \tag{C1}$$

$$Y(R) \equiv -\frac{2}{\pi}\int_0^{\pi/2} d\psi\, g'(\omega_0 + J_0 R\sin\psi)\sin\psi\cos^2\psi. \tag{C2}$$

$X(R) > 0$ follows from Eq. (C1), since we assumed $R > 0$. Integrating the right-hand side of Eq. (C2) by parts yields

$$Y(R) = -\frac{2J_0 R}{3\pi}\int_0^{\pi/2} d\psi\, g''(\omega_0 + J_0 R\sin\psi)\cos^4\psi. \tag{C3}$$

Here, we assume that $g''(x)$ exists. Note that $g'(\omega_0) = 0$ by definition. Since ω_0 is the unique maximum of $g(\omega)$, $g''(\omega) \leqslant 0$ follows. Thus, $Y(R) > 0$ since $R > 0$. Defining $\varepsilon \equiv \frac{J_1 R_1}{J_0 R}$ for $\varepsilon \ll 1$, from Eqs. (B12) and (B13), we obtain

$$R \simeq 2J_0 R\left(\frac{\pi}{2}X - \frac{\pi}{8}J_0 R\varepsilon^2 Y\right), \tag{C4}$$

$$R_1 \simeq 2J_1 R_1\left(X\frac{\pi}{4} - \frac{3\pi}{16}J_0 R\varepsilon^2 Y\right). \tag{C5}$$

When $\varepsilon = 0$, $R_1 = 0$. Let us set $R = R^*$ at $\varepsilon = 0$. Then, from Eq. (C4), we obtain

$$1 = \pi J_0 X(R^*). \tag{C6}$$

Thus, R^* satisfies Eq. (B1) for the U solution. Furthermore, from Eq. (C5), we obtain

$$R_1 \simeq 2\sqrt{\frac{R^*(J_1 - 2J_0)}{3\pi J_1^3 Y(R^*)}}. \tag{C7}$$

Since $Y(R^*) > 0$, we find that the Pn solution bifurcates from the U solution at $J_1 = 2J_0$ and exists when $J_1 > 2J_0$.

APPENDIX D: DERIVATIONS OF THE PHASE BOUNDARIES

1. Boundaries between the S and U phases

We will analyze the SCEs for the unstable Pn solutions (B20), (B21), and (B22) and derive the boundary between the S and U phases. Assuming $R \ll 1$, we can expand $A_{\theta'+\Theta_c-\Theta}$ into a Taylor series up to $O(R)$,

$$\begin{aligned} J_1 \bar{A}(\theta') \equiv A_{\theta'+\Theta_c-\Theta} &\simeq J_1 \bar{A}_0(\theta') + \frac{J_0 R_c\cos\theta'}{\bar{A}_0(\theta')}R, \\ \bar{A}_0(\theta') &= \sqrt{(R_c\cos\theta')^2 + (R_s\sin\theta')^2}. \end{aligned}$$

Thus, we obtain

$$\begin{aligned} g[\omega_0 + J_1\bar{A}(\theta')\sin\psi] \simeq\ & g[\omega_0 + J_1\bar{A}_0(\theta')\sin\psi] \\ & + g'[\omega_0 + J_1\bar{A}_0(\theta')\sin\psi] \\ & \times \frac{J_0 R_c\cos\theta'}{\bar{A}_0(\theta')}R\sin\psi. \end{aligned}$$

The SCEs become

$$R \simeq J_0 R Z_0 + J_1 R_c\langle\cos\theta'\rangle Z, \tag{D1}$$

$$R_c \simeq J_0 R\langle\cos\theta'\rangle_0 Z_0 + J_1 R_c\langle\cos^2\theta'\rangle Z, \tag{D2}$$

$$R_s \simeq J_1 R_s\langle\sin^2\theta'\rangle Z, \tag{D3}$$

$$\langle B\rangle_0 \equiv \frac{1}{Z_0}\frac{2}{\pi}\int_0^{\pi/2} d\psi\cos^2\psi \times \int_0^{\pi} d\theta' g[\omega_0 + J_1\bar{A}_0(\theta')\sin\psi]B, \tag{D4}$$

$$Z_0 \equiv \frac{2}{\pi}\int_0^{\pi/2} d\psi \cos^2\psi \times \int_0^{\pi} d\theta' g[\omega_0 + J_1\bar{A}_0(\theta')\sin\psi]. \quad \text{(D5)}$$

$\langle\cos\theta'\rangle_0 = 0$ holds, and by setting $R = 0$, Eqs. (D2) and (D3) lead us to $\langle\cos^2\theta'\rangle_0 = \langle\sin^2\theta'\rangle_0$. Thus, $R_c = R_s$ is satisfied on the boundary. Therefore, we have

$$\bar{A}_0(\theta') = R_c = \frac{R_1}{\sqrt{2}},$$
$$\bar{A}(\theta') \simeq J_1R_c + J_0R\cos\theta',$$
$$\langle B\rangle_0 = \frac{1}{Z_0}\frac{2}{\pi}\int_0^{\pi/2} d\psi\cos^2\psi\, g(\omega_0 + J_1R_c\sin\psi)\int_0^{\pi} d\theta' B,$$
$$Z_0 = 2\int_0^{\pi/2} d\psi\cos^2\psi\, g(\omega_0 + J_1R_c\sin\psi).$$

Thus, we obtain

$$\langle\cos\theta'\rangle \simeq \frac{1}{Z}\frac{2}{\pi}\int_0^{\pi/2} d\psi\cos^2\psi\int_0^{\pi} d\theta'(g(\omega_0 + J_1R_c\sin\psi) + g'(\omega_0 + J_1R_c\sin\psi)J_0R\cos\theta'\sin\psi)\cos\theta'$$
$$= \frac{1}{Z}J_0R\int_0^{\pi/2} d\psi\cos^2\psi\, g'(\omega_0 + J_1R_c\sin\psi)\sin\psi.$$

Equation (D1) becomes

$$R \simeq 2J_0R\int_0^{\pi/2} d\psi\cos^2\psi\, g(\omega_0 + J_1R_c\sin\psi) + J_0J_1RR_c \times \int_0^{\pi/2} d\psi\cos^2\psi\, g'(\omega_0 + J_1R_c\sin\psi)\sin\psi. \quad \text{(D6)}$$

Thus, on the boundary, we have

$$1 = 2J_0\int_0^{\pi/2} d\psi\cos^2\psi\, g(\omega_0 + J_1R_c\sin\psi) + J_0J_1R_c \times \int_0^{\pi/2} d\psi\cos^2\psi\, g'(\omega_0 + J_1R_c\sin\psi)\sin\psi. \quad \text{(D7)}$$

On the other hand, on the boundary, Eq. (D2) becomes

$$R_c = J_1R_c\langle\cos^2\theta'\rangle_0 Z_0 = J_1R_c\int_0^{\pi/2} d\psi\cos^2\psi\, g(\omega_0 + J_1R_c\sin\psi). \quad \text{(D8)}$$

This is nothing but the SCE (B3) for the stable S solution. Therefore, Eq. (D7) becomes

$$1 = 2\frac{J_0}{J_1} + J_0J_1R_c\int_0^{\pi/2} d\psi\cos^2\psi \times g'(\omega_0 + J_1R_c\sin\psi)\sin\psi. \quad \text{(D9)}$$

This can be rewritten as

$$J_0 = \left[\frac{2}{J_1} + J_1R_c\int_0^{\pi/2} d\psi \times g'(\omega_0 + J_1R_c\sin\psi)\cos^2\psi\sin\psi\right]^{-1}, \quad \text{(D10)}$$

which is the formula of the boundary between the S and U phases. We define $\hat{g}(x) \equiv \sigma g(\omega_0 + \sigma x)$, and consequently $\hat{g}'(x) = \sigma^2 g'(\omega_0 + \sigma x)$ follows. Defining $\bar{J}_i = \frac{J_i}{\sigma}$, we can rewrite Eqs. (D8) and (D10) as

$$R_c = \bar{J}_1R_c\int_0^{\pi/2} d\psi\cos^2\psi\,\hat{g}(\bar{J}_1R_c\sin\psi), \quad \text{(D11)}$$

$$\bar{J}_0 = \left[\frac{2}{\bar{J}_1} + \bar{J}_1R_c\int_0^{\pi/2} d\psi\,\hat{g}'(\bar{J}_1R_c\sin\psi)\cos^2\psi\sin\psi\right]^{-1}. \quad \text{(D12)}$$

If $g(\omega)$ is a Gaussian distribution with mean ω_0 and standard deviation σ, we have

$$\hat{g}(x) = \frac{1}{\sqrt{2\pi}}e^{-x^2/2}, \quad \hat{g}'(x) = -x\frac{1}{\sqrt{2\pi}}e^{-x^2/2}.$$

2. Boundary between S and Pn phases

The boundary between S and Pn phases is obtained from the SCEs for the unstable Pn solution by setting $R_c = 0$. Assuming $R_c \ll 1$, we can expand $\bar{A}(\theta')$ into a Taylor series up to $O(R_c)$. Defining $\hat{A}(\theta') = J_1\bar{A}(\theta')/\sigma$, we obtain

$$\hat{A}(\theta') = \sqrt{(\bar{J}_0R + \bar{J}_1R_c\cos\theta')^2 + (\bar{J}_1R_s\sin\theta')^2} \simeq \hat{A}_0(\theta') + \frac{\bar{J}_0\bar{J}_1RR_c\cos\theta'}{\hat{A}_0(\theta')},$$
$$\hat{A}_0(\theta') = \sqrt{(\bar{J}_0R)^2 + (\bar{J}_1R_s\sin\theta')^2}.$$

Accordingly, we have

$$g[\omega_0 + J_1\bar{A}(\theta')\sin\psi] \simeq g[\omega_0 + \sigma\hat{A}_0(\theta')\sin\psi] + g'[\omega_0 + \sigma\hat{A}_0(\theta')\sin\psi] \times \frac{\bar{J}_0\bar{J}_1RR_c\cos\theta'}{\hat{A}_0(\theta')}\sigma\sin\psi.$$

The SCE (B21) for R_c becomes

$$R_c \simeq \frac{2}{\pi}\int_0^{\pi/2} d\psi\cos^2\psi\int_0^{\pi} d\theta'\left(\hat{g}[\hat{A}_0(\theta')\sin\psi]\bar{J}_1R_c + \hat{g}'[\hat{A}_0(\theta')\sin\psi]\frac{(\bar{J}_0R)^2\bar{J}_1R_c}{\hat{A}_0(\theta')}\sin\psi\right)\cos^2\theta'. \quad \text{(D13)}$$

Thus, the boundary between the S and Pn phases is given by

$$1 = \frac{2}{\pi}\bar{J}_1\int_0^{\pi/2} d\psi\cos^2\psi\int_0^{\pi} d\theta'\left(\hat{g}[\hat{A}_0(\theta')\sin\psi] + \hat{g}'[\hat{A}_0(\theta')\sin\psi]\frac{(\bar{J}_0R)^2}{\hat{A}_0(\theta')}\sin\psi\right)\cos^2\theta'. \quad \text{(D14)}$$

On the other hand, on the boundary, the SCEs (B20) and (B22) for R and R_s become

$$R = \sigma\bar{J}_0R\frac{2}{\pi}\int_0^{\pi/2} d\psi\cos^2\psi\int_0^{\pi} d\theta' g[\omega_0 + \sigma\hat{A}_0(\theta')\sin\psi], \quad \text{(D15)}$$

$$R_s = \sigma\bar{J}_1R_s\frac{2}{\pi}\int_0^{\pi/2} d\psi\cos^2\psi \times \int_0^{\pi} d\theta' g[\omega_0 + \sigma\hat{A}_0(\theta')\sin\psi]\sin^2\theta'. \quad \text{(D16)}$$

Since $R_c = 0$ on the boundary, $R_1 = R_s$ holds. Furthermore, since the integrand is symmetric with respect to $\theta' = \frac{\pi}{2}$, changing the integral range from $[0,\pi]$ to $[0,\frac{\pi}{2}]$ and making a variable transformation $\theta' \to \frac{\pi}{2} - \theta''$ yields

$$R = \sigma \bar{J}_0 R \frac{4}{\pi} \int_0^{\pi/2} d\psi \cos^2\psi \times \int_0^{\pi/2} d\theta'' g[\omega_0 + \sigma \tilde{A}_0(\theta'')\sin\psi], \tag{D17}$$

$$R_1 = \sigma \bar{J}_1 R_1 \frac{4}{\pi} \int_0^{\pi/2} d\psi \cos^2\psi \times \int_0^{\pi/2} d\theta'' g[\omega_0 + \sigma \tilde{A}_0(\theta'')\sin\psi]\cos^2\theta'', \tag{D18}$$

$$\tilde{A}_0(\theta'') \equiv \hat{A}_0\left(\frac{\pi}{2} - \theta''\right) = \sqrt{(\bar{J}_0 R)^2 + (\bar{J}_1 R_1 \cos\theta'')^2}. \tag{D19}$$

These are merely the SCEs (B12), (B13), and (B14) for the stable Pn solution. Now, let us summarize the formulas of the boundary between the S and Pn solutions,

$$\bar{J}_1 = \left[\frac{4}{\pi}\int_0^{\pi/2} d\psi \cos^2\psi \int_0^{\pi/2} d\theta'' \left(\tilde{g}[\tilde{A}_0(\theta'')\sin\psi] + \tilde{g}'[\tilde{A}_0(\theta'')\sin\psi]\frac{(\bar{J}_0 R)^2}{\tilde{A}_0(\theta')}\sin\psi\right)\sin^2\theta''\right]^{-1}, \tag{D20}$$

$$R = \bar{J}_0 R \frac{4}{\pi} \int_0^{\pi/2} d\psi \cos^2\psi \times \int_0^{\pi/2} d\theta'' \tilde{g}[\tilde{A}_0(\theta'')\sin\psi], \tag{D21}$$

$$R_1 = \bar{J}_1 R_1 \frac{4}{\pi} \int_0^{\pi/2} d\psi \cos^2\psi \times \int_0^{\pi/2} d\theta'' \tilde{g}[\tilde{A}_0(\theta'')\sin\psi]\cos^2\theta'', \tag{D22}$$

$$\tilde{A}_0(\theta'') = \sqrt{(\bar{J}_0 R)^2 + (\bar{J}_1 R_1 \cos\theta'')^2}. \tag{D23}$$

APPENDIX E: DERIVATION OF THE SCEs FOR THE SPINNING SOLUTION AND PENDULUM SOLUTION FOR MODEL 2

In model 2, the interaction is given by

$$J_{\theta,\theta'} = \frac{1}{N}[J_m \cos\{m(\theta - \theta')\} + J_n \cos\{n(\theta - \theta')\}], \tag{E1}$$

where m and n are positive integers, and we assume $m < n$. Order parameters are defined as

$$R_{kc} e^{i\Theta_{kc}} = \frac{1}{N}\sum_\theta \cos(k\theta) e^{i\phi_\theta}, \tag{E2}$$

$$R_{ks} e^{i\Theta_{ks}} = \frac{1}{N}\sum_\theta \sin(k\theta) e^{i\phi_\theta}. \tag{E3}$$

k is m or n. As usual, we assume that R_{kc} and R_{ks} tend to be constant and $\Theta_{kc} \to \omega_0 t + \Theta'_{kc}, \Theta_{ks} \to \omega_0 t + \Theta'_{ks}$ as t tends to ∞, and Θ'_{kc} and Θ'_{kc} are constant. The evolution equation for ϕ_θ reduces to

$$\frac{d}{dt}\phi_\theta = \omega_\theta - A_\theta \sin(\phi_\theta - \omega_0 t - \alpha_\theta),$$
$$A_\theta e^{i\alpha_\theta} = \sum_{k=m,n} J_k[R_{kc}\cos(k\theta)e^{i\Theta'_{kc}} + R_{ks}\sin(k\theta)e^{i\Theta'_{ks}}]. \tag{E4}$$

Defining $\psi_\theta = \phi_\theta - \omega_0 t - \alpha_\theta$, the evolution equation becomes

$$\frac{d}{dt}\psi_\theta = \omega_\theta - \omega_0 - A_\theta \sin\psi_\theta. \tag{E5}$$

The order parameters are calculated as follows:

$$R_{kc} = \frac{1}{2\pi}\int_0^{2\pi} d\theta \int_{-\pi/2}^{\pi/2} d\psi\, n_s(\theta,\psi)\cos(k\theta)e^{i(\psi+\alpha_\theta-\Theta'_{kc})}, \tag{E6}$$

$$R_{ks} = \frac{1}{2\pi}\int_0^{2\pi} d\theta \int_{-\pi/2}^{\pi/2} d\psi\, n_s(\theta,\psi)\sin(k\theta)e^{i(\psi+\alpha_\theta-\Theta'_{ks})}. \tag{E7}$$

From these equations, we obtain

$$R_{kc} = Z\sum_{k'=m,n} J_{k'}[R_{k'c}\langle\cos(k'\theta)\cos(k\theta)\rangle e^{i(\Theta'_{k'c}-\Theta'_{kc})} + R_{k's}\langle\sin(k'\theta)\cos(k\theta)\rangle e^{i(\Theta'_{k's}-\Theta'_{kc})}], \tag{E8}$$

$$R_{ks} = Z\sum_{k'=m,n} J_{k'}[R_{k'c}\langle\cos(k'\theta)\sin(k\theta)\rangle e^{i(\Theta'_{k'c}-\Theta'_{ks})} + R_{k's}\langle\sin(k'\theta)\sin(k\theta)\rangle e^{i(\Theta'_{k's}-\Theta'_{ks})}]. \tag{E9}$$

Z and $\langle\cdot\rangle$ mean the same as before. That is,

$$\langle B\rangle = \frac{1}{Z}\frac{1}{\pi}\int_0^{\pi/2} d\psi \int_0^{2\pi} d\theta\, g(\omega_0 + A_\theta\sin\psi)\cos^2\psi\, B, \tag{E10}$$

$$Z = \frac{1}{\pi}\int_0^{\pi/2} d\psi \int_0^{2\pi} d\theta\, g(\omega_0 + A_\theta\sin\psi)\cos^2\psi. \tag{E11}$$

We further define R_k and φ_k by $R_{kc} + iR_{ks} = R_k e^{ik\varphi_k}$. For simplicity, we omit primes from the Θ's except for the expressions of α_θ ad ϕ^*_θ.

1. Spinning solution

First, let us study the spinning solution. We will assume $R_m > 0, R_n = 0$ and examine the auxiliary equations, which are the imaginary parts of Eqs. (E8) and (E9),

$$R_m \sin(m\varphi_m)\langle\cos(m\theta)\sin(m\theta)\rangle\sin(\Theta_{mc} - \Theta_{ms}) = 0, \tag{E12}$$

$$R_m \cos(m\varphi_m)\langle\cos(m\theta)\sin(m\theta)\rangle\sin(\Theta_{mc} - \Theta_{ms}) = 0. \tag{E13}$$

These equations are similar to Eqs. (A16) and (A17) in Appendix A. Therefore, for the stable S solution, $\cos(\Theta_{mc} - \Theta_{ms}) = 0$ and $\langle\cos(m\theta)\sin(m\theta)\rangle = 0$ follow, and

A_θ becomes

$$A_\theta = J_m\sqrt{[R_{mc}\cos(m\theta)]^2 + [R_{ms}\sin(m\theta)]^2} = J_m R_m\sqrt{\frac{1}{2}(1+\cos(2m\varphi_m)\cos(2m\theta))}. \quad \text{(E14)}$$

The SCEs are derived from the real parts of Eqs. (E8) and (E9).

$$R_{mc} = J_m R_{mc} Z\langle\cos^2(m\theta)\rangle, \quad \text{(E15)}$$

$$R_{ms} = J_m R_{ms} Z\langle\sin^2(m\theta)\rangle. \quad \text{(E16)}$$

$R_{mc} + iR_{ms}$ becomes

$$R_m e^{im\varphi_m} = J_m R_m Z[\cos(m\varphi_m)\langle\cos^2(m\theta)\rangle + i\sin(m\varphi_m)\langle\sin^2(m\theta)\rangle] \quad \text{(E17)}$$

and Eq. (E17) is rewritten as

$$1 = \tfrac{1}{2}J_m Z[1 + e^{-2im\varphi_m}\langle\cos(2m\theta)\rangle]. \quad \text{(E18)}$$

The real and imaginary parts of Eq. (E18) are

$$1 = \tfrac{1}{2}J_m Z[1+\cos(2m\varphi_m)\langle\cos(2m\theta)\rangle], \quad \text{(E19)}$$

$$0 = \tfrac{1}{2}J_m \sin(2m\varphi_m)\langle\cos(2m\theta)\rangle. \quad \text{(E20)}$$

Since in model 1, $R_c R_s \neq 0$ holds for the stable spinning solution, we assume that $R_{mc}R_{ms} \neq 0$. Thus, $\sin(2m\varphi_m) \neq 0$ and $\langle\cos(2m\theta)\rangle = 0$ follow from Eq. (E20). Therefore, we obtain $\cos(2m\varphi_m) = 0$ from Eq. (E14) and then $R_{mc} = R_{ms} = \frac{1}{\sqrt{2}}R_m, A_\theta = J_m R_{mc}$. Thus, Eq. (E19) becomes

$$1 = \tfrac{1}{2}J_m Z, \quad \text{(E21)}$$

that is,

$$1 = J_m\int_0^{\pi/2} d\psi\, g(\omega_0 + J_m R_{mc}\sin\psi)\cos^2\psi. \quad \text{(E22)}$$

This equation is the same as Eq. (29) for the stable spinning solution. The critical point is

$$J_m^{(c)} = J_1^{(c)} = \frac{4}{\pi g(\omega_0)} = 2J_0^{(c)}. \quad \text{(E23)}$$

The synchronized solution is

$$\alpha_\theta = \Theta_c' \mp m\theta,$$
$$\phi_\theta^* = \omega_0 t + \psi_\theta^* + \alpha_\theta = \omega_0 t + \sin^{-1}\left(\frac{\omega_\theta - \omega_0}{J_m R_{mc}}\right) + \Theta_c' \mp m\theta. \quad \text{(E24)}$$

The phase of the solution changes by $\pm 2\pi m$ when θ changes by 2π; that is, its rotation number is m.

2. Pendulum solution

Here, we assume $R_m R_n > 0$. From the imaginary part of Eq. (E8) with $k = m$ and the imaginary part of Eq. (E8) with $k = n$, we obtain

$$-J_m R_m \sin(m\varphi_m)\langle\cos(m\theta)\sin(m\theta)\rangle\sin(\Theta_{mc} - \Theta_{ms}) + J_n R_n[\cos(n\varphi_n)\langle\cos(m\theta)\cos(n\theta)\rangle\sin(\Theta_{nc} - \Theta_{mc}) + \sin(n\varphi_n)\langle\cos(m\theta)\sin(n\theta)\rangle\sin(\Theta_{ns} - \Theta_{mc}) = 0,$$
$$J_m R_m[\cos(m\varphi_m)\langle\cos(n\theta)\cos(m\theta)\rangle\sin(\Theta_{mc} - \Theta_{nc}) + \sin(m\varphi_m)\langle\cos(n\theta)\sin(m\theta)\rangle\sin(\Theta_{ms} - \Theta_{nc})] + J_n R_n\sin(n\varphi_n)\langle\cos(n\theta)\sin(n\theta)\rangle\sin(\Theta_{ns} - \Theta_{nc}) = 0. \quad \text{(E25)}$$

The sufficient conditions for these equations are that the coefficients of R_m ad R_n are 0. Accordingly, we obtain

$$\sin(m\varphi_m)\langle\cos(m\theta)\sin(m\theta)\rangle\sin(\Theta_{mc} - \Theta_{ms}) = 0, \quad \text{(E26)}$$

$$J_n R_n\sin(n\varphi_n)\langle\cos(n\theta)\sin(n\theta)\rangle\sin(\Theta_{nc} - \Theta_{ns}) = 0. \quad \text{(E27)}$$

For the pendulum solution, we assume $\sin(\Theta_{mc} - \Theta_{ms}) = 0$ and $\sin(\Theta_{nc} - \Theta_{ns}) = 0$ because similar conditions are obtained in model 1 for the stable Pn solution.

[The imaginary part of Eq. (E8) with $k = m$] + [$i\times$ the imaginary part of Eq. (E9) with $k = m$], and [the imaginary part of Eq. (E8) with $k = n$] + [$(-i)\times$ the imaginary part of Eq. (E9) with $k = n$] reduce to

$$\sin(\Theta_{nc} - \Theta_{ms})\langle e^{im\theta\cos(\Theta_{mc}-\Theta_{ms})}\cos\{n(\theta' - \tilde{\theta})\}\rangle = 0, \quad \text{(E28)}$$

$$\sin(\Theta_{nc} - \Theta_{ms})\langle e^{in\theta\cos(\Theta_{nc}-\Theta_{ns})}\cos(m\theta')\rangle = 0. \quad \text{(E29)}$$

Here, we define

$$\bar{\theta}_k = \varphi_k e^{i(\Theta_{kc}-\Theta_{ks})} = \varphi_k\cos(\Theta_{kc} - \Theta_{ks}),$$
$$\tilde{\theta} = \bar{\theta}_n - \bar{\theta}_m, \quad \theta' = \theta - \bar{\theta}_m.$$

We assume that $\sin(\Theta_{nc} - \Theta_{ms}) \neq 0$. From the real and imaginary parts of Eq. (E28), we obtain

$$\langle\cos(m\theta)\cos\{n(\theta' - \tilde{\theta})\}\rangle = 0, \quad \text{(E30)}$$

$$\langle\sin(m\theta)\cos\{n(\theta' - \tilde{\theta})\}\rangle = 0. \quad \text{(E31)}$$

From the real and imaginary parts of Eq. (E29), we obtain

$$\langle\cos(n\theta)\cos(m\theta')\rangle = 0, \quad \text{(E32)}$$

$$\langle\sin(n\theta)\cos(m\theta')\rangle = 0. \quad \text{(E33)}$$

[Equation (E30) + $i\times$ Eq. (E31)] and [Eq. (E32) + $i\times$ Eq. (E33)] reduce to

$$\langle e^{im\theta'}\cos\{n(\theta' - \tilde{\theta})\}\rangle = 0, \quad \text{(E34)}$$

$$\langle e^{in\theta'}\cos(m\theta')\rangle = 0, \quad \text{(E35)}$$

where θ has been replaced with $\theta' + \bar{\theta}_m$. From Eq. (E35), we obtain

$$\langle\cos\{(m+n)\theta'\} + \cos\{(n-m)\theta'\}\rangle = 0, \quad \text{(E36)}$$

$$\langle\sin\{(m+n)\theta'\} + \sin\{(n-m)\theta'\}\rangle = 0. \quad \text{(E37)}$$

On the other hand, by using Eq. (E35), Eq. (E34) reduces to

$$\langle\sin\{(n-m)\theta' - n\tilde{\theta}\}\rangle = 0. \quad \text{(E38)}$$

$A_\theta = A_{\theta'+\bar{\theta}_m}$ is expressed as

$$A_{\theta'+\bar{\theta}_m} = ((J_m R_m)^2\cos^2(m\theta') + (J_n R_n)^2\cos^2\{n(\theta' - \tilde{\theta})\} + J_m J_n R_m R_n\cos(\Theta_{nc} - \Theta_{ms})\cos(\Theta_{mc} - \Theta_{ms}) \times \{\cos(n\tilde{\theta})[\cos\{(m+n)\theta'\} + \cos\{(n-m)\theta'\}] + \sin(n\tilde{\theta})[\sin\{(m+n)\theta'\} + \sin\{(n-m)\theta'\}]\})^{1/2}. \quad \text{(E39)}$$

$\cos(\Theta_{nc} - \Theta_{ms})\cos(n\tilde{\theta}) = 0$ and $\cos(\Theta_{nc} - \Theta_{ms})\sin(n\tilde{\theta}) = 0$ follow from Eqs. (E36) and (E37). That is,

$$\cos(\Theta_{nc} - \Theta_{ms}) = 0. \quad \text{(E40)}$$

Therefore, we obtain

$$A_{\theta'+\tilde{\theta}_m} = \sqrt{[J_m R_m \cos(m\theta')]^2 + [J_n R_n \cos\{n(\theta' - \tilde{\theta})\}]^2}. \tag{E41}$$

$\langle\cos\{(m+n)\theta'\}\rangle = 0$ and $\langle\sin\{(m+n)\theta'\}\rangle = 0$ follow from Eq. (E41) because $n \neq m$. Thus, Eqs. (E36) and (E37) reduce to

$$\langle\cos\{(n-m)\theta'\}\rangle = 0, \tag{E42}$$

$$\langle\sin\{(n-m)\theta'\}\rangle = 0. \tag{E43}$$

Therefore, Eq. (E38) is satisfied. If $n \neq 3m$, conditions (E42) and (E43) are automatically satisfied. For simplicity, we will assume $n \neq 3m$. Thus, the conditions for Pn are

$$\sin(\Theta_{mc} - \Theta_{ms}) = 0, \quad \sin(\Theta_{nc} - \Theta_{ns}) = 0, \quad \cos(\Theta_{nc} - \Theta_{ms}) = 0. \tag{E44}$$

Now, let us study the SCEs, which are the real parts of Eqs. (E8) and (E9). [The real part of Eq. (E8) with $k = m$] + [$i\times$ the real part of Eq. (E9) with $k = m$] and [the real part of Eq. (E8) with $k = n$] + [$i\times$ the real part of Eq. (E9) with $k = n$] give the SCEs,

$$1 = \frac{J_m Z}{2}\langle 1 + e^{2im\theta'\cos(\Theta_{mc}-\Theta_{ms})}\rangle, \tag{E45}$$

$$1 = \frac{J_n Z}{2}\langle 1 + e^{2in(\theta'-\tilde{\theta})\cos(\Theta_{nc}-\Theta_{ns})}\rangle. \tag{E46}$$

The real and imaginary parts of Eq. (E45) are

$$1 = J_m Z\langle\cos^2(m\theta')\rangle, \tag{E47}$$

$$\langle\sin(2m\theta')\rangle = 0. \tag{E48}$$

The real and imaginary parts of Eq. (E46) are

$$1 = J_n Z\langle\cos^2\{n(\theta' - \tilde{\theta})\}\rangle, \tag{E49}$$

$$\langle\sin\{2n(\theta' - \tilde{\theta})\}\rangle = 0. \tag{E50}$$

Equation (E48) is automatically satisfied since $\tilde{A}_{\theta'}$ does not contain the factor $\sin(2m\theta')$. From Eq. (E50), we have

$$\langle\sin(2n\theta')\rangle\cos(2n\tilde{\theta}) = \langle\cos(2n\theta')\rangle\sin(2n\tilde{\theta}). \tag{E51}$$

The sufficient condition for this is $\cos(2n\tilde{\theta}) = 0$ or $\sin(2n\tilde{\theta}) = 0$, and it determines the value of $\tilde{\theta}$.

Therefore, the SPEs are

$$1 = J_m Z\langle\cos^2(m\theta)\rangle, \tag{E52}$$

$$1 = J_n Z\langle\cos^2\{n(\theta' - \tilde{\theta})\}\rangle. \tag{E53}$$

By changing the variable from θ to θ', the SPEs can be expressed as

$$1 = \frac{J_m}{\pi}\int_0^{\pi/2} d\psi \int_0^{2\pi} d\theta' g(\omega_0 + A_{\theta'+\tilde{\theta}_m}\sin\psi) \times \cos^2\psi\cos^2(m\theta'), \tag{E54}$$

$$1 = \frac{J_n}{\pi}\int_0^{\pi/2} d\psi \int_0^{2\pi} d\theta' g(\omega_0 + A_{\theta'+\tilde{\theta}_m}\sin\psi) \times \cos^2\psi\cos^2\{n(\theta' - \tilde{\theta})\}, \tag{E55}$$

where $A_{\theta'+\tilde{\theta}_m} = \sqrt{[J_m R_m \cos(m\theta')]^2 + [J_n R_n \cos\{n(\theta' - \tilde{\theta})\}]^2}$. Setting $\bar{\alpha}_\theta = \alpha_\theta - \Theta_{ms}$, we have

$$A_\theta \cos\bar{\alpha}_\theta = J_m R_m \cos(\Theta_{mc} - \Theta_{ms})\cos(m\theta'), \tag{E56}$$

$$A_\theta \sin\bar{\alpha}_\theta = J_n R_n \sin(\Theta_{nc} - \Theta_{ms})\cos\{n(\theta' - \tilde{\theta})\}. \tag{E57}$$

Thus,

$$\phi_\theta^* = \omega_0 t + \sin^{-1}\left(\frac{\omega_\theta - \omega_0}{A_\theta}\right) + \bar{\alpha}_\theta + \Theta'_{ms}. \tag{E58}$$

This formula shows that the rotation number can take on values of $0, \pm 1, \ldots, \pm m$.

[1] D. S. Saunders, *An Introduction to Biological Rhythms* (Blackie, Glasgow, 1977).
[2] A. T. Cloudsley-Thompson, *Biological Clocks—Their Function in Nature* (Weidenfeld and Nicolson, London, 1980).
[3] A. T. Winfree, J. Theor. Biol. **16**, 15 (1967).
[4] Y. Kuramoto, *Chemical Oscillations, Waves, and Turbulence* (Springer-Verlag, Berlin, 1984).
[5] Y. Kuramoto, in *Proceedings of the International Symposium on Mathematical Problems in Theoretical Physics*, edited by H. Araki (Springer, New York, 1975).
[6] H. Sakaguchi, S. Shinomoto, and Y. Kuramoto, Prog. Theor. Phys. Lett. **77**, 1005 (1987); Y. Kuramoto and H. Nakao, Phys. Rev. Lett. **76**, 4352 (1996).
[7] H. Daido, Phys. Rev. Lett. **68**, 1073 (1992).
[8] J. P. L. Hatchett and T. Uezu, Phys. Rev. E **78**, 036106 (2008); J. Phys. Soc. Jpn. **78**, 024001 (2009).
[9] R. E. Mirollo and S. H. Strogatz, J. Stat. Phys. **60**, 245 (1990); S. H. Strogatz and R. E. Mirollo, *ibid.* **63**, 613 (1991); R. E. Mirollo and S. H. Strogatz, J. Nonlinear Sci. **17**, 309 (2007).
[10] Y. Kuramoto and I. Nishikawa, in *Cooperative Dynamics in Complex Physical Systems*, edited by H. Takayama (Springer, Berlin, 1989), p. 300.
[11] H. Chiba and I. Nishikawa, Chaos **21**, 043103 (2011).
[12] E. Ott and T. M. Antonsen, Chaos **18**, 037113 (2008); **19**, 023117 (2009).
[13] E. A. Martens, E. Barreto, S. H. Strogatz, E. Ott, P. So, and T. M. Antonsen, Phys. Rev. E **79**, 026204 (2009).
[14] D. Pazó and E. Montbrió, Phys. Rev. E **80**, 046215 (2009).
[15] Y. Kuramoto and D. Battogtokh, Nonlinear Phenom. Complex Syst. **5**, 380 (2002).
[16] S. I. Shima and Y. Kuramoto, Phys. Rev. E **69**, 036213 (2004).
[17] C. R. Laing, Physica D **238**, 1569 (2009); Chaos **19**, 01311d (2009); Phys. Rev. E **81**, 066221 (2010).
[18] J. N. Teramae and D. Tanaka, Phys. Rev. Lett. **93**, 204103 (2004).
[19] D. S. Goldobin and A. Pikovsky, Phys. Rev. E **71**, 045201 (2005).
[20] H. Nakao, K. Arai, and Y. Kawamura, Phys. Rev. Lett. **98**, 184101 (2007).
[21] K. Nagai, H. Nakao, and Y. Tsubo, Phys. Rev. E **71**, 036217 (2005).

[22] H. Nakao, K. S. Arai, K. Nagai, Y. Tsubo, and Y. Kuramoto, Phys. Rev. E **72**, 026220 (2005); K. Arai and H. Nakao, *ibid*. **77**, 036218 (2008).

[23] J. A. Acebrón, L. L. Bonilla, C. J. Pérez Vicente, and F. Ritort, Rev. Mod. Phys. **77**, 137 (2005).

[24] M. Antoni and S. Ruffo, Phys. Rev. E **52**, 2361 (1995).

[25] A. Campa, T. Dauxois, and S. Ruffo, Phys. Rep. **480**, 57 (2009), and papers cited therein.

[26] T. Uezu, T. Kimoto, and M. Okada, J. Phys. Soc. Jpn. Lett. **81**, 073001 (2012).

[27] D. H. Hubel and T. N. Wiesel, J. Physiol. **160**, 106 (1962); **195**, 215 (1968).

[28] D. Ruelle and F. Takens, Commun. Math. Phys. **20**, 167 (1971).

[29] T. Kimoto, T. Uezu, and M. Okada, J. Phys. Soc. Jpn. **80**, 074005 (2011).

[30] T. Uezu, T. Kimoto, and M. Okada, J. Phys. Soc. Jpn. **81**, 064001 (2012).